Light-induced excited spin-state trapping : a methodological approach

Guillaume Chastanet, Cédric Desplanches, Mathieu Gonidec, Philippe Guionneau, Mathieu Marchivie, Corine Mathonière, Patrick Rosa

Comprehensive Coordination Chemistry III

Light-Induced Excited Spin-State Trapping: a Methodological Approach

Guillaume Chastanet, Cédric Desplanches, Mathieu Gonidec, Philippe Guionneau, Mathieu Marchivie, Corine Mathonière, Patrick Rosa

All authors belong to: CNRS, Univ. Bordeaux, ICMCB, UMR5026, F-33600 Pessac, France

Correspondence: guillame.chastanet@icmcb.cnrs.fr, nathalie.daro@icmcb.cnrs.fr, cedric.desplanches@icmcb.cnrs.fr, mathieu.gonidec@icmcb.cnrs.fr, philippe.guionneau@icmcb.cnrs.fr, mathieu.marchivie@icmcb.cnrs.fr, corine.mathoniere@icmcb.cnrs.fr, patrick.rosa@icmcb.cnrs.fr

Abstract

Light-Induced spin state state switching has been widely studied over the last 40 years, exploring the different time and size scales. This exploration was performed by using a wide range of techniques which are still growing in resolution and accuracy to face the challenge of the increasing complexity of the studied materials (multifunctionnality, nanoparticles, thin films, single domain, single molecule…). All these techniques are well described in various papers and reviews emphasizing their specificities and richness. The aim of the chapter is to discuss most of these techniques from a methodological point of view in order to be aware of all the cautions to take while using them. The most usual techniques used to induce and record the light-induced spin crossover will be described, complemented by a series of recommendations to be in the best conditions for such measurements. The informations that could be extracted or not from these techniques will also be presented in order to have the right level of interpretation.

Keywords

Photoswitching, light-induced spin crossover, electron transfer, vibrational spectroscopy, optical spectroscopy and reflectivity, magnetometry, X-Ray diffraction, Synchrotron radiation.

INTRODUCTION

Switchable molecules and materials constitute an important class of systems which properties can be modulated by external stimuli. Among the wide range of sytems it includes, this chapter is only devoted to the Spin Crossover (SCO) and electron transfer (ET) phenomena in molecule-based materials. However, most of the techniques we discuss here and related requierements could be applied to other light-sensitive switches. The interest of light lies on its ability to be selective, affording reversibility of the light-induced switching. Moreover, it operates on an ultrafast time scale since the photoswitching can be achieved within one picosecond. The combination of a fast and selective tool with fast optical readout of the spin state, opens the way to ultrafast data manipulation.

Among the different available perturbations, temperature and light are probably the most commonly used. While the temperature can basically be viewed as a source of energy that allows electrons to be promoted from the t_{2g} orbitals to e_g in an ideal octahedral coordination sphere, light can act in different ways. Light excitation can be adjusted to specific electronic transitions (*d-d*, Metal-Ligand Charge Transfer, *MLCT*, Ligand-Metal Charge Transfer -*LMCT*- or Ligand-Ligand Charge Transfer –*LLCT*-…).[1] Moreover, when ligand photoreactions are induced by light, ligand conformation changes can occur (photo-isomerization or cyclization), consequently tuning the ligand field and the global SCO behavior. This is at the core of the Ligand-Driven Light-Induced Spin Change (LD-LISC)[2] and the Light-Driven Coordination-Induced Spin-State Switching (LD-CISSS)[3] phenomena. When the wavelength matches metallic *d-d* absorption bands or *MLCT* transitions, some transient excited states can be populated leading to trapping of a metastable state as in the widely studied Light-Induced Excited Spin-State Trapping (LIESST) effect.[4] Finally, light may act as a source of heat deposited onto the material. Depending on the number of photons, strong heating may occur, leading to photo-thermal effects that allow the occurrence of spin crossover, especially in hysteretic materials.[5]

Regarding the electron transfer (ET) phenomenon it implies the presence of electronic donor and acceptor moieties to promote a reversible transfer of one electron (or more) between two sites through temperature change and/or photoexcitation at low temperature. In addition, this ET can be associated with a spin crossover process. As for SCO materials, the modification of the electronic configuration by light irradiation allows magneto-optical bistability. Different donor/acceptor couples have been considered in molecular compounds, such as radicals or complexes, implying an electron transfer between an organic moiety (radical/ligand)[6] and a metal center or between two metal ions.[7] Basically, when one electron is transferred from one metal to another (or to an organic ligand, as occurs e.g. in valence tautomerism), the oxidation state of the metals changes. This change is associated with an electronic reorganization leading to SCO. A topical question related to these systems is whether the charge transfer triggers the spin state switching or the other way around.[8]

Due to the numerous changes occuring within the SCO and ET processes, there are many ways to trigger the spin state switching (table 1).[1,9,10,11,12] Magnetic characterizations such as vibrating sample magnetometry or SQUID magnetometry follow the magnetic change. Vibrational spectroscopies (FTIR, Raman) and X-Ray diffraction probe the change in the metal-ligand bond length. The color change is followed by absorption (of light or X-Rays) or reflectivity measurements. Mössbauer probes both the spin state and degree of oxidation of iron-based compounds. Calorimetric experiments (DSC) gives insights on the thermodynamical characteristics of the materials. X-Ray absorption close to the metal edge will provide information on oxidation and spin states (XANES) and structural data (EXAFS). These are the most common techniques used to characterized SCO and ET switching. As far as the technical environment allows it, these characterizations could be performed under light irradiation. However, one has to be conscious that, depending on the techniques, the temperature regulation systems differ from one set-up to the other, leading to possible variation in the temperature range of observation of the thermally-induced phenomena such as the thermally-induced spin crossover and the relaxation processes.

The objectives of this chapter are to describe how to perform such light-induced characterizations using optical and vibrational techniques, magnetic measurements and X-Ray diffraction. A last part will be devoted to surface measurements since such switchable materials are increasingly considered in electronic devices in which nanoparticles or thin films are used. To lay foundations to these parts, the first section will present the basics of light-induced spin crossover.

Changes	Techniques
Spin state	Magnetism, Mössbauer, XANES
Optical properties	Absorption spectroscopy, Reflectivity
Oxidation state	Mössbauer, Magnetism, XANES
Structural changes	X-Ray diffraction, EXAFS, Vibrational spectroscopies (IR, Raman)
Phase transition	Calorimetry

Table 1. *The most common techniques used to follow the property changes associated with spin crossover and electron transfer phenomena.*

1. Light-Induced Spin Crossover

As mentioned in the introduction, there are several ways to induce a spin crossover by light irradiation. The most common one is related to the LIESST process. When photon energy is tuned in resonance with absorption bands of the metal complex, it can induce the electronic spin state switching of the system. For example, in Fe(II) complexes, transition from the LS-singlet state to the HS-quintet state involves intermediate excited states and intersystem crossings. The photo-physical processes have been investigated by different techniques to evidence the mechanism at play but the aim of this chapter is not to present them since several reviews have been written in that sense.[1,4,13] In the last 35 years the description of the LIESST phenomenon has evolved from a classical double potential wells picture of the energy as function of the isotropic bond-length elongation to a more complex three dimensional view accounting for the anisotropy of the elongation (Figure 1). For Fe(II) compounds, absorption of the LS state around 500 nm corresponds to the $^1A_1 \rightarrow {}^1T_1$ transition followed by a cascade between excited states with at least two intersystem crossings of $\Delta S = 1$ each. The kinetics of each step of the cascade have been widely investigated through time-resolved experiments leading to a precise description of the spectroscopy of the LIESST effect.[13c,14] In most compounds, the *d-d* band of the metal center might be masked by a more intense MLCT band involving a charge transfer between the metal and the ligand close to half an electron charge.[15] In some cases, irradiation in the HS state absorption band around 830 nm corresponding to the $^5T_2 \rightarrow {}^5E$ transition may lead to the reverse-LIESST process and back population of the initial LS state.[16] For ET systems, irradiation is set to MMCT band to promote the metal-metal electron transfer and its wavelength obviously depends on the metals implied in the process. It appears obvious that, prior to any light-induced spin crossover experiment on a given compound, its optical signature should be recorded in order to identify the appropriate irriadiation wavelength.

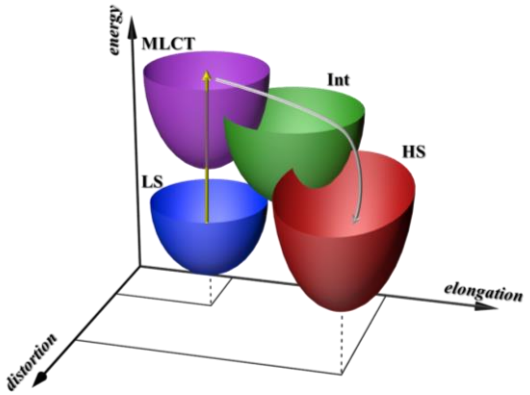

Figure 1. *3D view of the HS, LS and some excited vibrational potential wells as a function of elongation and distortion.*

In the following parts the most usual techniques used to induce and record the light-induced spin crossover will be described, complemented by a series of recommendation to be in the best conditions for such measurements. The informations that could be extracted or not from these techniques will also be presented in order to have the right level of interpretation.

2. Optical and vibrational measurements on crystals and powders

2.1. Vibrational spectroscopies

Several studies have been devoted to vibrational spectroscopies applied to the spin crossover phenomenon. Reviews have been written on the subject.[11,17] The use of vibrational spectroscopies such as infrared (IR) and Raman techniques to probe the electronic configuration of a given compound is based on the change in metal-ligand bond-length along the spin crossover or the electron transfer. In the particular case of iron-based spin crossover compounds, one consequence is that the Fe(II)-ligand stretching vibrations are shifted by as much as 200 cm^{-1}, making these stretching vibrations useful to characterize the spin state of the Fe(II) ion. Other vibrations of the ligands are also affected by the spin crossover. One classical example is given by the shift in the N-(CS) stretching of the NCS^- ligand during HS to LS conversion. For $[Fe(phen)_2(NCS)_2]$, these vibration frequencies vary from 2062-2074 cm^{-1} for HS to 2107-2114 cm^{-1} for LS.[18] Beyond the simple determination, of the spin state, IR and Raman spectroscopies are very useful tools for time-resolved or spatially resolved studies of SCO systems. We will not develop these remarkable techniques already described in review articles.[11,17b] The rest of this paragraph will rather focus on some experimental critical points when IR or Raman spectra are used to study SCO compounds. For each of these critical points, a typical example issued from the literature will be given.

The two major techniques for recording an IR spectra are the so-called ATR (Attenuated Total Reflectance) mode and the transmission mode. The spin crossover complex $[Fe(3ditz)_3](BF_4)_2$ has been used as a model system to compare advantages and drawbacks of these two modes for IR spectroscopy.[19] According to the article, "*in the Mid-IR spectra, the transmission mode is the clear favorite, as it combines a satisfying temperature range with good spectral quality and signal intensities over the full temperature and spectral range. The ATR accessory allows for lower temperatures and faster heating/cooling cycles, but suffers from weaker signal intensities, ice formation in the low-temperature range and interferences in the high temperature range*". As far as Far-IR is concerned, it seems that the comparison is slightly in favor of ATR, as it avoids the matrix effects (polyethylene for example) especially at low temperature.

When using the transmission mode, a transparent sample should be prepared. One classical technique used to prepare a sample for IR spectroscopy is to grind a small amount of sample with a specially purified salt, usually potassium bromide KBr. It has to be emphasized that this way of preparing the sample can be a problem when SCO compounds are studied. Indeed several SCO systems have shown to be sensitive to grinding. Often, grinding the sample results in a spin conversion being more partial than for the initial sample resulting for example in a higher HS fraction at low temperature. An example has been observed with $[Fe(3\text{-}OCH_3\text{-}SalEen)_2]PF_6$.[20] This modification of the SCO behavior has been attributed to defects caused by grinding. Another similar example has been observed on $[Fe(4,7\text{-}(CH_3)_2phen)_2(NCS)_2]\cdot\alpha$-pic.[21] Grinding the sample with MgO powder has resulted in a strong narrowing of the thermal hysteresis loop. For a 1D spin crossover polymer $[FeL(4,4'\text{-bipy})]_n$, a surprising effect has been observed. The compound was shown to be purely HS under the form of crystals and to present a SCO behavior when ground (Figure 2).[22] This

uncommon behavior has been attributed to a too rigid packing of the molecules in the crystals except on the surface which is more flexible. Grinding the sample increases the ratio surface/bulk sample, leading for the most finely ground powders to a complete spin transition.

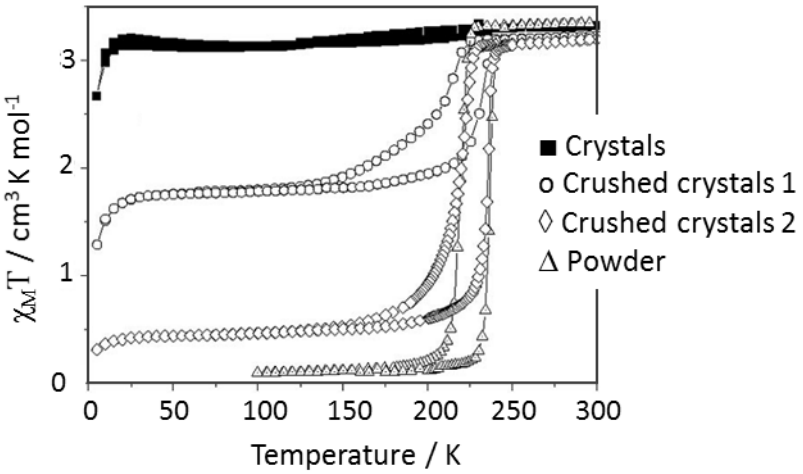

Figure 2. *Thermal variation of $\chi_M T$ product for different samples of compound [FeL(4,4'-bipy)]$_n$: magnetic properties of the crystals (solid squares), pulverised crystals (open circles and open squares) and a separately prepared powder sample (triangles). Adapted from ref 22.*

Another effect to account for when preparing a sample as a KBr pellet is the amount of pressure that is applied. When a KBr pellet is prepared, the applied pressure is typically between 500 and 1000 MPa. However, smaller pressures have been shown to modify strongly and irreversibly the spin crossover properties. For examples, XRD data were recorded before and after pressure was applied and released on single-crystals of [Fe(PM-PEA)$_2$(NCS)$_2$].[23] Following the temperature dependence of the unit-cell parameter *a*, a thermal hysteresis of 19 K is observed at ambient pressure (0.1 MPa) whereas this hysteresis width is 63 K after a pressure of 20 MPa has been applied and released (Figure 3).

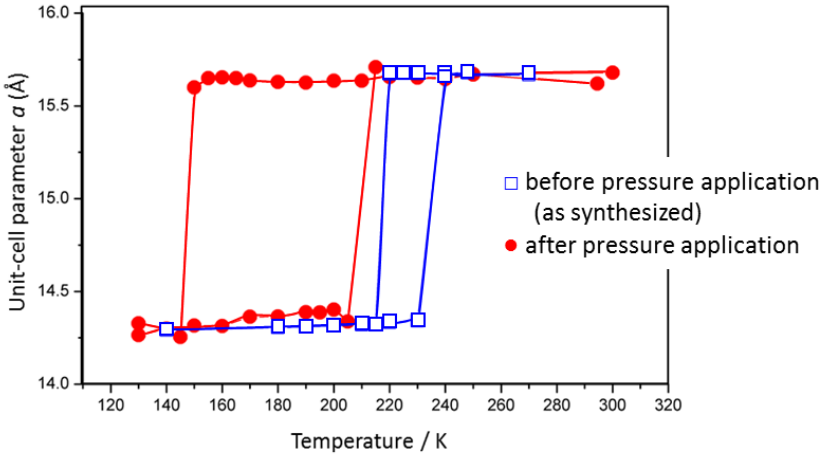

Figure 3*. Temperature dependence of the unit-cell parameter a for [Fe(PM-PEA)$_2$(NCS)$_2$] for a crystal as-synthesized (empty blue square) and after the crystal was submitted to a pressure of 20 MPa (filled red circle). Adapted from ref 23.*

In addition to sample preparation precautions, IR and Raman techniques have their own constraints. In science, it should always be remembered that any measurement can possibly perturb

the studied system. This is typically the case of the vibrational spectroscopies that use a laser irradiation as probe that can perturb the sample's behavior either by inducing the LIESST effect at low temperature or by heating the sample, as examplified below.

Herber et al. studied the "guinea pig" spin crossover system $[Fe(phen)_2(NSC)_2]$ thanks to FT-IR spectroscopy.[24] The LS fraction of the sample has been monitored following the infrared absorbance at 2114 and 2106.5 cm^{-1} of the N-(CS) stretching mode of the NCS^- ligand. The thermal spin crossover was reproduced, although there was a clear difference in the inflexion point of the infrared absorption (~ 159 ± 5 K) and the transition temperature reported earlier (175 ± 1 K), mainly following from the sample preparation as mentioned above. In addition, at temperature below 70 K, the He/Ne laser (632.8 nm) of the IR spectrometer is able to populate the HS state of the compound through the LIESST effect, preventing the observation at lower temeprature of the pure LS state. Thus great care should be taken when IR is recorded at low temperature where LIESST effect could be effective. The LIESST effect can also be observed by Raman spectroscopy. The $[Fe(Hpy-DAPP)](BF_4)_2$ has been studied by Raman spectroscopy between 78 and 300 K using a laser excitation at 632.8 and 785 nm.[25] While the 785 nm wavelength allows to observe the pure LS state, use of the 632.8 nm wavelength results in a constant photoexcitation, in a pump-probe situation, preventing thus the observation of the LS state at all temperatures. This example shows that not only the laser of the Raman spectrometer is able to perturb the system, but that the choice of a given wavelength can be crucial. Confocal Raman experiments were conducted on the $[Fe(Htrz)_2(trz)](BF_4)$ spin crossover polymeric compound presenting a thermal hysteresis of about 40 K.[26] Outside the thermal hysteresis, the continuous Raman-probe laser produce a stationary HS fraction as long as the irradiation is maintained. As soon as the power of the laser is reduced, the LS spin state is recovered. On the other hand, it has been possible thanks to the Raman-probe laser to switch permanently a fraction of the compound in its high spin state when the irradiation takes place in the thermal hysteresis loop.[5c,g] Unlike the case described in the previous paragraph, the formation of the HS state is not due to the LIESST effect but to the heating of the sample by the laser. This was confirmed by taking advantage of the spatial resolution of the Raman microscope. Indeed, the local heating induces around the laser spot a partial LS to HS conversion.

2.2. UV-Visible absorption spectroscopy

UV-visible absorption spectroscopy is an analytical technique that has been extensively used for coordination compounds, in particular as an efficient tool for helping in the elucidation of their electronic structures.[27] SCO and ET compounds have been therefore extensively studied by this spectroscopy. They can be studied in solutions (aqueous or organic solvents) and also in the solid state. The solid state spectra can be measured on single crystals when they are big enough or as powders diluted in a transparent matrix (ie. KBr or $BaSO_4$) or in films (cf. §5).

The analysis of the optical spectra allows getting crucial information for the understanding of the spin crossover systems, because in principle the determination of the crystal field splitting is possible. Experimental spectra consist of several d-d transitions, and when dealing with octahedral complexe the use of Tanabe-Sugano diagram helps for the estimation of the crystal field (Δ) and Racah (B) parameters. This approach is well explained for the $[Fe(ptz)_6](BF_4)_2$ complex[28] that is known to change from a white color in its low spin (LS) state to a red color in its high spin (HS) state (Figure 4). The spectrum of the HS state is made of one spin-allowed d-d transition $^5T_2 \rightarrow {}^5E$ around 11800 cm^{-1} that gives directly the value of Δ, whereas the spectrum of the LS state obtained at low temperature contains two spin-allowed d-d transitions associated to $^1A_1 \rightarrow {}^1T_1$ and $^1A_1 \rightarrow {}^1T_2$,

respectively. Δ has been estimated at 19140 cm^{-1} and B as 740 cm^{-1}. In a more general picture, the optical studies are helpful to estimate the crystal field range, and then to predict for a given complex if it can display (or not) a spin crossover. Given that the electron pairing energy Π ≈ 15,000 cm^{-1} for the Fe(II) ion, SCO is possible when $\Delta^{HS} < \Pi < \Delta^{LS}$ and not possible when $\Delta^{HS} < 10{,}000\ cm^{-1}$ or $\Delta^{LS} > 23000\ cm^{-1}$.

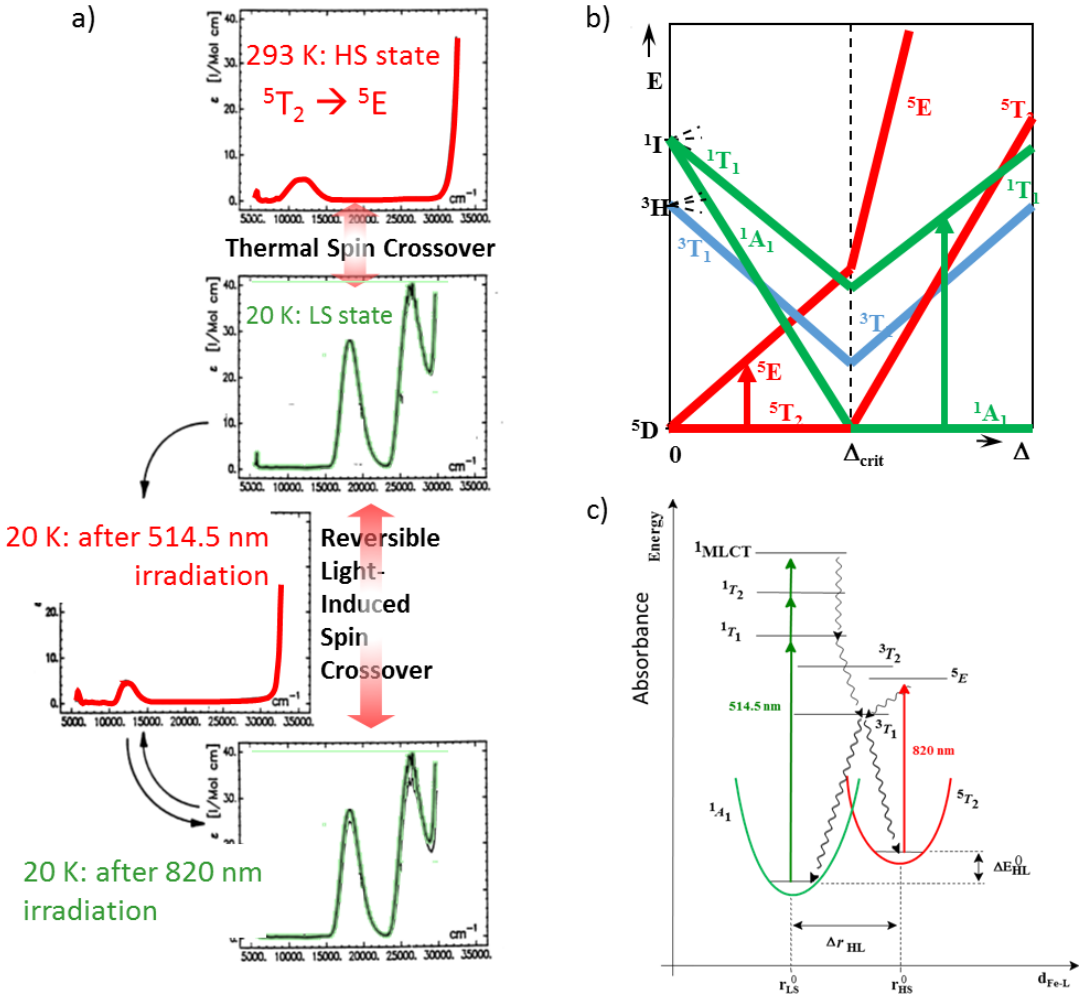

Figure 4*. (a) Optical spectra of single crystals of $[Fe(ptz)_6](BF_4)_2$ complex at room temperature (HS state, red), at 20 K before irradiation (green), after irradiation at 514.5 nm at 20 K (red) and after irradiation at 820 nm (green). (b) Tanabe Sugano diagram for the Fe(II) d^6 configuration and the corresponding transitions (red for the HS state at 273 K and at 20 K + hυ; green for the LS state). Adapated from ref 29. (c) energy diagram of the LS and HS potential wells and the corresponding transitions.*

The ideal situation for revealing the thermochromic behaviour of a system is the realization of the optical study in temperature on single crystals (Figure 4). In addition, the photochromic behavior associated to the LIESST effect can be also followed during the same experiment, as soon as an external optical source delivering green light (510-530 nm range) is available during the experiment. For instance, electronic spectra have been used to discover the LIESST effect in the $[Fe(ptz)_6](BF_4)_2$ complex. Actually, green light irradiation of the crystal at low temperature allows the observation of crystals of white color having a spectrum comparable to the one recorded at room temperature

(Figure 4) revealing without ambiguity the photo-induced formation of the HS state.[29] Moreover, the high-spin → low-spin relaxation processes can be studied by optical spectroscopy to follow the decay of the $^5T_2$ → ^5E optical absorption.[29] Recently, optical studies of a 2D coordination network $\{Fe(bbtr)_3(BF_4)_2\}_\infty$ reveal a peculiar behaviour that is the persistent bidirectional optical switching around 65 K giving rise to a true light-induced bistability.[30]

There is a large family of SCO Fe(II) compounds containing aromatic nitrogen-based ligands like 4,4'-bipyridine or similar ligands possessing moderate π-back bonding effect. In these cases, the optical spectra are strongly dominated by symmetry-allowed electronic transitions like MLCT (Metal ligand Charge Transfer) transitions, that hide the weakly intense symmetry-forbidden d-d transitions. Therefore the direct estimation of the crystal field parameters is not easy, or even impossible. An elegant approach is to study isostructural Ni(II) complexes for which the low-energy d-d transition appearing in the near-infrared region gives the direct determination of the crystal field parameters.[31] Shatruk et al. have recently reapplied this strategy to estimate the effect of a ligand functionalization on crystal field strengths in a family of Ni(II) complexes.[32] A similar trend is expected for the Fe(II) analogues, and this is nicely confirmed by their magnetic properties.

Solution UV-visible absorption spectroscopy can be also used to monitor SCO in solutions, ie. above the freezing point of common solvents.[33] But the LIESST is only observable at low temperature (T < 100 K). Therefore, to observe a light-induced spin change of a molecular species at room temperature (or close to the room temperature), two approaches have been developed, namely the LD-LISC[2] and the LD-CISSS[3]. In both cases, the insertion in the complex of a photoactive (or photoisomerizable) ligand triggers a spin change by structural reorganization in the coordination sphere of the complex. In the case of the LD-LISC this reorganization occurs not too close from the metal centers modifying slightly the electronic density around the metal center, and then the spin state. For the LD-CISSS, the coordination sphere of the metal center is strongly modified due to the photo-induced increase in the coordination number (CN) inducing a different geometry around the metal center (for instance from square planar with CN = 4 to a square pyramidal geometry with CN = 5). Both phenomena have been studied by solution and solid state UV-visible absorption spectroscopy.

2.3. Optical reflectivity spectroscopy

The optical contrasts generated by the thermochromic and the photochromic behaviours of SCO and ETcompounds are quite important in the visible range, as evidenced by absorption spectroscopy (see above). Consequently, both are easy to detect, even with a simple optical set-up. Researchers have developed home-made optical spectroscopy set-up based on reflectivity instead of absorption (Figure 5a).[34] The advantages of this surface technique is (i) the possibility to use a small quantity of powders (< 5 mg) instead of single crystals, (ii) the minimization of the cost to obtain cryogenic temperatures (T down to 10 K), (iii) the study of the wavelength-excitation dependency of the photo-induced properties, and also the easy realization of cycles (photo-excitation and de-excitation). An example of a complete reflectivity study on a new Fe(II) mononuclear compound is shown on Figures 5b-d. The observed optical effects are then confirmed by photomagnetic measurements.[35]

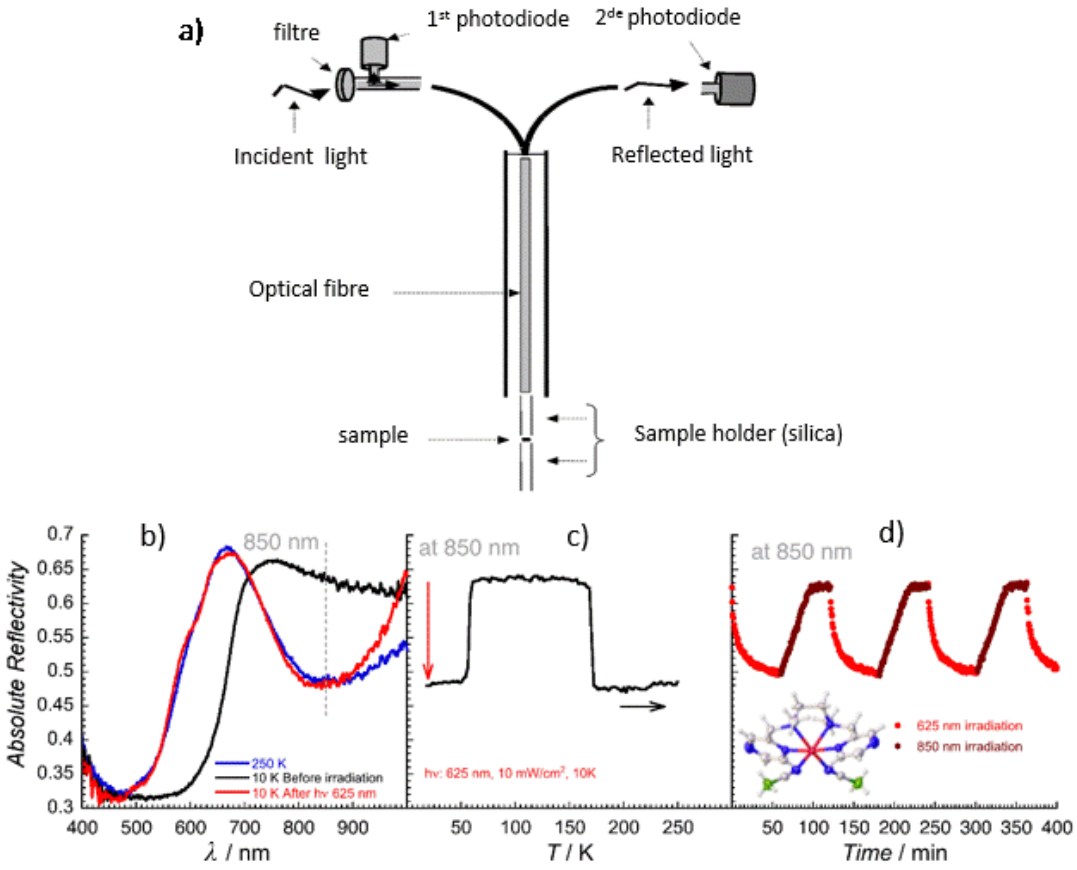

Figure 5. *(a) Optical reflectivity set-up from ref 34. (b) Comparison of the reflectivity spectra at 250 K, at 10 K before irradiation and after 625-nm irradiation for [Fe(Lpz)(NCBH$_3$)$_2$] complex. (c) Thermal variation of the reflectivity signal recorded at 850 nm increasing the temperature in dark at 4 Kmin^{-1} after irradiation by a 625-nm LED at 10 K for 30 min. (d) Time evolution of the reflectivity signal at 850 nm under successive irradaitions at 10 K by 625-nm (red) and 850-nm LEDs showing the good reversibility.*[35]

Reflectivity set-ups differ depending on the temperature range of measurement. From room temperature to 10 K, one can use either the easily accessible low-cost option of temperature-stratification inside a liquid helium dewar or a more expensive active optical cryostat (flow or closed-cycle). In the former case the sample is simply moved into a helium atmosphere, stratified above the liquid helium in the dewar. This stratification is stable and allows an accurate temperature control. The sample is then only exposed to helium atmosphere below room temperature. This is in contrast with active cryostat where usually the sample is exposed to vacuum. When higher temperatures are required – from 100 to 500 K for instance – liquid nitrogen-based set-ups can be used instead. Such an apparatus requires the use of a closed cryostat to work under vacuum. Therefore, for very pressure-sensitive compounds or solvated samples, such experiment could affect both the switching temperature and the composition (desolvation). Finally, for higher temperature range – above room temperature – a temperature controlled stage device could be used to finely control the temperature.[36] One just has to be sure that the sample remains stable in the investigated temperature range. In addition, reflectivity measurements have been used in pump-probe time-resolved experiments, especially to evidence the multistep mechanism underlying the LS → HS photoswitching.[5b,e,g,h,i,14]

An additional caution that has to be taken regards the probe light source. As for vibrational spectroscopies, the probe light can induce the LIESST effect at low temperature preventing any observation of the pure LS state. To avoid this, a stroboscopic probe should be used.

3. Magnetic characterizations on crystals and powder

The photomagnetic properties of switchable compounds are investigated using SQUID magnetometers, typically Quantum Design MPMS systems. The measurement is based on the motion over a few centimetres (extraction over the 4 cm of maximum field homogeneity) of a sample into a magnetic field leading to induced current in a second-order gradiometer that is detected by a supraconducting Josephson junction tuned as a resonant circuit by a RF bias. To have an accurate signal, the sample and its environment over the extraction area should be as close as possible to symmetry by translation. To shine light onto the sample, an optical fiber is brought through the sample rod close to the sample. Two approaches may be used to insure a symmetric signal. The first one consists in keeping the optical fiber farther than the 4 cm of the extraction (typically 6 cm) so that the signal induced by the fiber does not perturbate the sample's signal. The other strategy consists in placing the fiber so that its extremity is almost in contact above the sample and to introduce a piece of fiber below the sample in order to keep the symmetry of the setup.

The SQUID magnetometry records the volumic properties of the sample. However, since light irradiation is involved in the LIESST process, obviously, light penetration depth has to be maximized; *i.e.* the sample preparation must lead to the deepest penetration of light into the sample. To do so, samples are prepared as thin layers. Powder or crystals can be deposited on a piece of double-face scotch tape, or sealed in a small plastic bag (typically polyolefins). By doing so, between 0.1 to 1 mg are typically used. This has several consequences.

The first one is the difficulty to measure accurately the mass of the sample. One possibility to obtain it is to calculate it by comparing the thermal spin crossover curve recorded on this sample with the one obtained on a more accurately weighed sample of the same material. The other one is obviously to weigh the sample using a microbalance accurate to at least 0.01 mg. In all cases, the diamagnetic correction of the sample holder has also to be estimated, depending on the way it is prepared (see below).

A second consequence of such a preparation using so small an amount of sample is the weakness of the magnetic signal. Centring of the signal in the SQUID magnetomer is then crucial, especially since at low temperature, before irradiation, compounds are usually diamagnetic, often with a magnetic contribution of the same order of magnitude than the sample holder. One way to obtain proper centring is to perform it under irradiation, when the paramagnetic state is populated, and keep it for the whole measurement, typically by not using the *Iterative Regression* algorithm in Quantum Design MPMS magnetometers. Indeed, this algorithm induces another difficulty regarding the diamagnetic to paramagnetic transition that induces a negative to positive signal change. Therefore, since the magnetic signals in the initial and final states are of opposite sign, during the photo-excitation and relaxation processes the signal irremediably passes through zero, leading to possibly wrong centring if the centre has not been fixed before.

Specific sample preparation could be required in case of compounds sensitive to the primary vacuum in the sample chamber of the SQUID magnetometer. This is typically the case of solvated compounds. Samples can be either embedded in grease (which adds a significant diamagnetic contribution) or sealed in transparent bags. However, whatever the sample preparation, in some

cases the opacity of the sample is so strong that it prevents efficient light penetration. Photo-excitation is thus incomplete, and the sample can be considered as bi-phasic with a top-phase at the surface fully photoexcited, and a bottom phase practically unexcited. Such a situation can also be observed when the absoption properties of the compound strongly change upon light-conversion, leading to a change in the light irradiation efficiency. This is typical of a bleaching effect that could lead to non-linear photo-excitation features as well as inhomogeneity[37]. Such an inhomogeneity of photo-excitation has to be taken into account when the studied material is cooperative, as the relaxation activation energy is a function of the photo-excited fraction. Optimization of light excitation requires determination of the absorption spectra of the two states involved. For a deeply coloured compound, it was shown that the photo-excitation is more efficient in the shoulder of an absorption band than at the maximum.[38]

Moreover, since light brings energy, it warms the sample. As a consequence, usually the magnetic signal decreases (in the absence of strong magnetic interactions, as it is usually the case in most SCO compounds, the sample follows the classical Curie law). The intensity should be adjusted to prevent too much heating of the sample and temperature instability. Such heating effects can be probed by switching off the light and recording the magnetic signal. If a jump in the signal is observed at the same recorded temperature it means that light has locally heated the sample. One has to compromise between small heating effects and efficiency of irradiation.

Finally, light penetration may be also strongly dependent on the morphologies of the sample grains. Microstructural studies, altough yet rare, have demonstrated how the size and shapes of the grains of a SCO material may differ, depending on the synthesis.[39] For LIESST measurements, one probably has to favour homogeneous and regular shapes together with small sizes.

4. Crystallographic measurements on crystals and powder

While we are dealing with a topic as challenging as obtaining structural data on a sample in a photo-excited state, we must first ask ourselves the question of the purpose of the experiment. "*The end justifies the means*" is an adage attributed to the Renaissance humanist thinker Nicolas Machiavelli that, if applied here at the first degree - which was certainly not the original idea - can be transposed to the situation described below in this paragraph: the means used depend on and are justified by the purpose of the investigation process. Depending on the goal of the photo-crystallography experiment, the methodology can vary greatly, ranging from an almost routine experience to a pioneering investigation in crystallography. The relevance of structural analysis, particularly by diffraction, conducted on SCO materials is demonstrated daily and has been the focus of detailed reviews in recent years.[10,40] Similarly, the usefulness of structural analysis of photo-excited states is well illustrated in the SCO literature.[41] The purpose here is not to go back over these aspects but to report on the specific methodological features required to get reliable structural data on samples in photo-excited states.

We will focus here-after mainly on X-Ray Diffraction. All the instructions usually given in numerous manuals, books and articles to obtain reliable structural data under standard experimental conditions by this approach remain valid and will not be recalled here; this includes instructions for the experiment as well as the data analysis.[42]

4.1 Preparing the experiment

First of all, as said above, before any experiment in photo-crystallography, it is important to determine its purpose. The range of information that can be obtained by X-ray diffraction is very

wide, and the determination of atomic positions (full crystal-structure) allows to know the state of spin, but also to discuss the topologies of the interactions within the atomic architecture and the associated symmetries - information that is crucial for describing the properties of SCO materials. But, even in this case, the expected subtlety of the desired description must be anticipated in terms of resolution. High resolution experiments (*i.e.* below the standard 0.8 Å) will require a peculiar attention to the stability of the rate of photo-conversion all over the experiment. Indeed, any variation in the conversion rate would have a dramatic effect on the quality of the final structure, which is all the more sensitive as high precision is wanted. Note that outstanding atomic resolutions have already been obtained for the description of the structural properties of SCO materials in photo-excited states, raising the feasibility of such an approach.[15,43] It is clear that the feasibility of a high-resolution experiment should first be tested by such a study in the LS state at low temperature before attempting it in photo-excited conditions. On the one hand, this approach will provide an element of comparison, on the other hand it can be very relevant in terms of time saving since it will make it possible to set the experimental conditions specific to the crystal being investigated. A structural analysis may also not aim for a complete determination but, for example, simply to know the metric and symmetry of the crystal unit-cell. In this case, a partial and therefore rapid registration is sufficient, which makes it less difficult to maintain the conversion rate throughout the experiment. For example, one of the major recurring questions asked is whether the symmetry of the unit-cell in the photo-excited state is similar to that of the high temperature HS state, the HS state after quenching or the LS state. In this case, a rapid investigation may be considered. Note that while the crystalline symmetry of the metastable HS* state is often identical to that of the high temperature HS state, differing cases have also been reported.[40a,41a] Time dependent structural studies of the LIESST effect require a specific methodology and are specifically addressed below. In addition, if microstructural scale information is wanted, the preparation of the experiment should consist in minimizing instrumental contributions to Bragg-peak profiles. This probably requires a lot of preliminary testing on the device used.

Of course, the choice of the X-rays source is crucial. High-resolution experiments with laboratory sources are possible but synchrotron sources allowing very quick data collection should be preferred if difficulties in stabilizing the photo-excited states during a few hours is anticipated. The X-ray wavelength should be chosen taking into account the above purpose of the investigation but also by considering a possible action of X-rays on the photo-conversion itself. It has been shown that, in some cases, soft and hard X-rays from synchrotron sources can populate metastable HS states leading to the excited spin-state; this refers to SOXIESST and HAXIESST effects (see *section 5* for discussion on the occurrence of these effects on surface).[44]

The optical source features (wavelength, power, collimation and thus fluence) should be chosen from optical and photo-magnetic investigations, as described above in *sections 2 and 3.*, with the aim of maximizing the conversion rate. The photo-crystallography experiment must then be attempted once photo-magnetic data are available; reversing this order can lead to very significant time losses and even erroneous conclusions due to a wrong choice of optical sources. A possible warming of the crystal due to the laser irradiation should be anticipated and, if possible, tested by preliminary trials. In structural analysis, careful examinations of ellipsoids may allow to reach the actual temperature of the sample.[45] The optical source must be placed near the sample such as it does not perturb the XRD data collection - *i.e.* it must not interfere with the goniometer and detectors motions - in a position that allows irradiating the sample at any time during the experiment, for reasons developed below.

The temperature of data collection and overall the whole warming and cooling protocol must be chosen from the photomagnetic data and the structural study of the thermal SCO. However, the lowest reachable temperature must be privileged when possible since very low temperature is favorable to a high rate of photo-conversion, a good stability of the conversion[43] and a better signal-to-noise ratio in XRD data.[45b]

The single-crystal dimensions and morphology must be chosen to facilitate a full photo-conversion. Clearly, small (thin) samples with few facets are preferable. At least, the sample must not be larger than the laser beam diameter. Even though the first crystal structure of a SCO compound in its HS photo-excited state was determined with a single crystal glued on a glass fiber,[41h] it is highly suggested not to glue it. The SCO is very often accompanied by large volume modifications[10,40] that can induce macroscopic cracks on the crystal especially if part of the latter is glued. The use of cryoloops to mount the crystal within the X-ray and optical beams is recommended; the drop of oil on the loop being as small as possible not to perturb the light irradiation and therefore the photo-conversion rate. For the same reason the oil must be chosen as transparent as possible - paratone-N is suitable for example. The specificity of powder sample preparations is discussed below.

The structural properties of the crystalline sample must be carefully checked prior to any low temperature experiment in the optical irradiation environment. At least, the LS and HS crystal structures must be perfectly known and it is highly recommended to also determine the crystal structures at the temperature the photo-experiment is planned for both the LS and the quenched HS states. These data appear to be crucial when determining the exact conversion rate into the crystal for instance. Of course, since polymorphism is highly frequent in SCO compounds,[10,40,46] it is mandatory to perform a full data collection before light irradiation on the crystal investigated to check this aspect.

The course of the low temperature XRD experiment in light irradiation conditions is often unexpected and many events can interrupt the data collection (crack of the sample, spin-state relaxation, shutdown of the X-ray beam/laser/detector/cryostat, icing ... and so on ...) which can be dramatic in the context of long duration photo-excitation experiments, especially if few samples are available. With that idea in mind, one has to first target the main goal of the experiment before investigating further points, *i.e.* first perform the full data collection at the lowest temperature under irradiation before investigating potential warming effects if the main goal is to determine the atomic positions in the HS* state.

Once the above points are clear (scheme 1), the experiment can start; the first goal being to reach the photo-excited state.

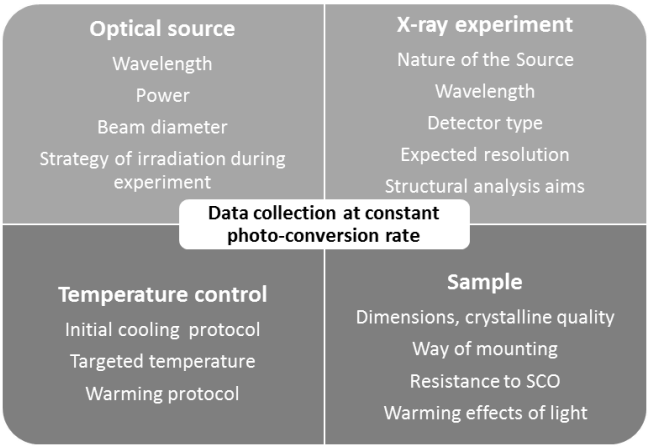

***Scheme 1**. Short checklist of various aspects to be anticipated or known prior to any photo-crystallography experiment aiming at the investigation of photo-excited states. See text for some possible methodological choices.*

4.2 Reaching the photo-excited state with the highest conversion rate

Undoubtedly, the main methodological objective during a photo-crystallography experiment on an SCO compound is to obtain the best conversion rate on the sample before any data recording. It has been shown that a low conversion rate can have dramatic consequences on data quality. For example, a 4% population of species in a different spin state than the targeted one can affect the Fe—N bond lengths by more than three standard deviations.[43a] The general idea is to bring the sample to the lowest possible temperature - it depends on the cryostat available but generally it is around 10-20 K - so that it is in the LS state, and then to irradiate with the laser to convert toward the HS state. However, several cooling strategies can be used. Indeed, it is well known that cooling kinetics can strongly influence the HS →LS conversion rate and that, sometimes, crystals can be damaged by thermal SCO.[10,40,47] In this case, a slow cooling from room temperature to the experimental temperature is not the best choice. It is recommended to first quench the sample directly at 10 K (or the lowest available temperature). In this case, the crystal is in a quenched HS state which, incidentally, may also prove interesting to study. Then, it is slowly heated until it converts to the LS state, the latter being controlled by a measurement of the unit-cell for example. Finally, once the crystal is in the LS state, it is cooled back to 10K (scheme 2). On should not forget to switch off the indoor light of the diffractometer all along this process.

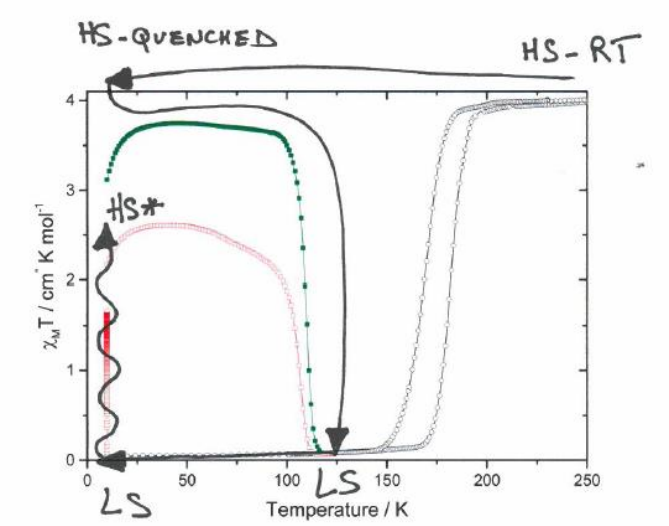

***Scheme 2**. Best cooling methodology to reach the photo-excited state without damaging the crystal, in most cases. See text for restrictions.*

The cooling methodology described above is the one that generally gives the best conversion rate while preserving the diffracting qualities of the sample. However, a few points should be clarified. First of all, this requires a good prior knowledge of the photomagnetic behavior, including the T(LIESST) temperature, and the structural properties of the sample in the HS and LS states. Secondly, this method is only possible if the cryostat allows a true quenching. The difference between quenching and fast cooling has already been described.[48] The use of a cryostat with helium jet allows a real quenching when a closed cryostat allows a very fast one. For some samples, rapid cooling will be sufficient to reach the quenched HS state. Thirdly, this methodology is only possible if

the temperature range offered by the cryostat allows the quenched-HS state to the LS conversion. It may be that this conversion occurs at a temperature too high for the capacities of the cryostat using helium. Since slow cooling is not always possible, it appears that, puzzlingly, samples with the highest T(LIESST) values are the most difficult to characterize on a photo-crystallography experiment, as the cryostat does not necessarily allow a good conversion rate to be obtained.

Whatever the cooling method chosen - slow cooling or *via* quenching - the lowest temperature should be preferred for the final step. Once the sample is in the LS state at the lowest temperature, the crystal is then irradiated to obtain the photo-excited HS* state. The X-ray diffraction probes the sample by volume. It is important that the entire sample is photo-excited to get a homogenous LS to HS* conversion on the whole sample. As mentioned before, the choice of the crystal dimensions is therefore important for this step, as is the choice of laser power - these aspects are sample dependent and must be pre-tested. From a methodological point of view, it is necessary to rotate the crystal within the laser beam in order to irradiate all its faces.

4.3 Keeping the sample-state stable all along the data collection

The structural investigation of the photo-excited HS state, HS*, should be done normally with the laser off. However, the XRD data collection can be long and, apart from laser excitation, some of the complexes in the HS* state could relax to the LS state during the data recording, which would be dramatic for the final quality of the crystal structure and could even make the data set unusable. It is to prevent this HS*--> LS relaxation that it has been advised above to work at the lowest possible temperature. If this is not enough - again preliminary tests must be carried out to anticipate this aspect - then it is possible to regularly stop the XRD data collection, put again the laser ON and rotate continuously the crystal to (re)populate the HS*; then switch OFF the laser and continue the XRD data collection. This alternation between the optical and X-ray irradiations of the sample must ensure a negligible HS* to LS relaxation but of course it must be used with great care to control the homogeneity of the collected Bragg intensity sets.

Obviously, the formation of ice around the crystal must be avoided more than ever in this type of experiment because not only can it disturb the collection of diffraction intensities but it can also hinder the light irradiation of the sample. In this respect, the use of closed cryostats has a clear advantage.

Another possibility is to perform the XRD data collection under continuous laser irradiation. The good point is to limit or even cancel the HS* to LS relaxation, which greatly improves the final quality of the crystal structure. The bad point is that this method necessarily causes a significant increase in the sample temperature. Crystals irradiated by a laser at very low temperatures can indeed undergo a significant increase of temperature. Knowing the true temperature of the sample is then crucial in the structural analyses step as well as in the structure-properties relationships discussions. A usual method in crystallography to estimate the temperature of the crystal is based on the determination of the average isotropic temperature factor of the atoms within the crystal structure using the so-called Wilson plot of the Bragg intensities.[49] However, it has been demonstrated that the case of SCO compounds is quite puzzling since the value of the temperature factor is strongly biased by the partial LS to HS* conversion rate, the possible HS* to LS relaxation as well as the distortion generated by the SCO itself.[43a] Therefore, knowing the true temperature in photo-excited SCXRD experiments for SCO compounds remains a challenge.

Clearly, keeping in mind the idea to perform a data collection on a sample with a stable HS* fraction, a synchrotron beam line environment is favourable, though not at all mandatory, since it shortens considerably the time of data collection.

4.4 The specific case of powders

The main specificity in powders cases comes from the difficulty of irradiating efficiently by laser the entire sample probed by X-rays that penetrate deeper than visible light into the sample. In a standard powder X-ray diffraction (PXRD) experiment, the required sample volume is much larger than the possibility of full photo-conversion offered by a laser irradiation and the risk is that only the surface of the sample is indeed in the photo-excited state. As a result, the PXRD pattern must be analysed as a mixture of HS* and LS phases which can, in certain cases, correspond to a great limitation for reliable results. Note that once again it depends on the expected purpose of the experiment (see above). This difficulty is even larger if the powder is within a close cycle cryostat. The frame of the latter perturbs a lot the PXRD pattern, without speaking of the difficulties to keep a flat surface for the sample in such environment, because of vacuum. A flat sample surface is required in PXRD experiments to avoid biases that are difficult to correct in the subsequent Rietveld refinement. Other problems come from the possible gradient of temperature on the powder sample. This must be anticipated by a good knowledge of the cryostat used - which is a general thought. More specifically, SCO powders may also show preferential orientation induced by the strong modification of the unit-cell parameters at the spin-crossover. This aspect, once again, may be anticipated by a careful investigation of the thermal SCO prior to the photo-crystallography one.

Considering all the possible problems mentioned above, the best solution for getting reliable results on SCO powders in the photo-excited state is probably to use capillaries as sample holders.[44c] PXRD using capillaries allows using only a few grains - which is favorable here for an efficient photo-conversion by light - and is suitable with open flow cryostats, limiting most of the above problems. Absorption corrections - required in case notably of intended Rietveld refinements - and instrumental contributions to Bragg-peaks widths must then be perfectly known prior to the experiment. Another possibility is to work on monolayer powders, *i.e.* using grazing incidence. In such cases, the structural information will concern microstructural aspects mainly. Elsewhere, the use of neutron diffraction offers many advantages for powder study of photo-excited states at very low temperature since the use of a closed cryostat does not disturb the measurement in any way.

4.5 Further remarks

Time-resolved investigation of the LIESST effect has proved to be powerful and recently brought remarkable advances on the understanding of the mechanism of the SCO phenomenon.[10,41d,50] Structural studies of the SCO on a time scale of seconds or minutes can be approached with a classical methodology, described above. On the contrary, dealing with ultrafast processes - typically at the femto- or nano scales - requires a very high level of expertise and know-how that is still very rare since owned by only a few persons worldwide. This delicate methodology is based on a combination of diffraction (X-ray, electron) and spectroscopy techniques. It requires short X-ray pulses as offered by synchrotrons and X-FELs that has, in fact, a specific methodology for obtaining reliable structural data. Note however that, even in that case, the main methodological problems are the same as those described above and concern the level and the stability of the photo-excited state during the X-ray data collection - which is mainly achieved by using stroboscopic methods as suggested in *section 4.2*.

In summary, the methodology of a LIESST experiment in photo-crystallography combines the usual difficulties of any structural analysis together with the major challenge of maintaining a constant (and highest) conversion rate throughout the data recording. From a methodological point of view, the structural study of the LIESST effect becomes a pioneering experiment when it combines laser irradiation with another constraint than low temperature, such as the application of pressure for example. This latter combination is clearly a perspective in the SCO field. Similarly, it is clear that the quality of the information obtained in this type of non-routine investigation increases with the data quality, in this respect the use of image analysis methods such as the maximum entropy method would be a significant step forward in the field.

5. Measurement on surfaces

Amongst recent developments in the study of Spin Crossover compounds, the preparation of films, down to the submonolayer scale, and their characterization, have figured prominently. The study of those films has included the possibility of photoexciting them. Nevertheless, when working at that scale problems are numerous, starting from the preparation of the films themselves, their morphology and the nature of the deposited species, the behaviour of the film as compared to the original properties of the bulk molecule, and then of course the study of the effect of incident light. Characterization techniques are limited due to the necessary high sensitivity required by the minute amount of compound actually present in the film. On the other hand, one immediate advantage when working with thin films is the expected improvement in photoexcitation due to the negligible absorption of the incident light by the reduced amount of molecules in the film.

5.1 Preparation and characterization

The recent flurry of publications on the preparation of spin crossover thin films has led to various reviews establishing the state of the art in the various methods available to obtain such films.[51] The oldest reported method followed the Langmuir-Blodgett (LB) approach, with molecules modified by grafting long hydrophobic alkyl chains in order to ensure phase separation at a the air/water interface. After compression one obtains well-organized monolayers that can be transferred on a flat substrate such as glass or a polymer.[52,53] Nevertheless the necessary chemical modification, that can drastically affect the spin crossover properties, has severely limited the extension of this method. A more recent approach, consists in building spin-crossover architectures by performing on-surface chemical synthesis.[54] This approach has essentially been limited so far to coordination networks, and perhaps the most striking results are those involving sequential layer-by-layer (LBL) growth methods.[55] In this case, the surface is “initialized” through chemical grafting of a precursor, then successive reactions with chemicals constituting the building blocks of the final network allow to control the growth of the thin film to the desired thickness.[55c] This approach has also been followed to obtain designed monolayers.[56] Other "wet" chemistry methods, that is drop-casting, micro-contact printing, and spin-coating have been reported in a few examples.[50b,c] Spin-coating is a method of choice in molecular electronics for the preparation of organic thin films of controlled thickness, it is thus all the more surprising that its use with SCO compounds has been so limited, but this may be due to the complications in obtaining continuous smooth films. Last but not least is physical vapour deposition (PVD), the thermal sublimation of SCO complexes onto a substrate of choice. Though quite restricted, since it imposes charge neutrality and restrictions on mass of the compounds to be evaporated, this latter method allows clean preparations of thin films, which greatly facilitates their subsequent study.

The effective build-up of the film may be followed or checked by a variety of techniques, either in operando, such as the Quartz Crystal Microbalance (QCM) routinely used in PVD setups, or the use of sensors in solution such as a Surface Plasmon Resonance (SPR) or QCM sensors that can follow the adsorption of successive layers in a LBL experiment, or ex situ, where all Scanning Probe Microscopies (SPMs) are usually the tools of choice to follow the build-up of the film, then to check its morphology: continuity, roughness, orientation... Thickness can be checked either with the presence of a step, or using X-ray based techniques such as X-Ray Reflectometry. Morphology and thickness are not directly relevant for the study of photoactive SCO species, as we will see further on, but one should stress that for in-depth physical studies related to potential applications of such films, they are usually key parameters. For example the reliability of molecular electronics devices is highly dependent on getting smooth continuous films of controlled thicknesses.

5.2 Surface-analysis techniques

The methods mentioned above present different avenues for the deposition or anchoring of SCO compounds on surfaces, but for a variety of reasons, it is far from guaranteed that the compounds present on the surface after the deposition or grafting process are chemically intact. For starters, Fe(II) compounds can easily get oxidized, and the high surface-area/volume ratio in thin films can exacerbate problems with the stability of the compounds that are not necessarily observable in the bulk. Layer-by-layer methods proceed via a different pathway than classical homogenous solution reactions and therefore may generate intermediate species with unknown stabilities. And finally PVD-based methods require to heat the molecules to rater high temperatures and in those conditions it is not rare to observe degradation of the compound in the sublimation step or to have a cleavage of the compound on the surface due to the reactivity of the surface itself. For all of those reasons, before proceeding to characterizing the functionality of the films, it is important to check first the chemical nature and integrity of the molecules constituting the film, with techniques requiring increasing sensitivity with decreasing thickness. The currently used techniques can be either quantitative or qualitative. Spectroscopic techniques are usually non-destructive. Since those techniques can in most cases also be used to quantify states in photoactive SCO thin films, we will briefly review them.

5.2.1 Mass spectrometry

Special emphasis must be put upon Time-of-Flight Secondary Ion Mass Spectrometry (ToF-SIMS).[57] This technique, using a primary beam of heavy ions (typically Ar^+, Au^+, C_{60}^+…) bombarding the surface, analyzes with a time-of-flight detector the secondary ions produced, and manages sensitivities down to the submonolayer. Most of those secondary ions originates from the top 1-2 nm of the film. The technique does not allow a full chemical analysis, since the spectra pattern are dependent on the molecule-substrate interactions and of course the ionization yields. Nevertheless careful comparison of the complex fragmentation patterns usually obtained with related bulk and/or thick films samples can support the preservation of the molecule of interest in the thin film, though without allowing to exclude partial degradation.[57] Moreover, the technique is destructive since it ablates the film during the analysis, but although this could be seen as a disadvantage it also means that analyzing the fragmentation patterns with time allows to obtain compositional depth profiles. A last advantage of this technique lies in its spatial resolution, down to 100 nm, a feature of choice for example in the case of stamped/printed patterns.

5.2.2 Vibrational spectroscopies

Beyond mass spectrometry, vibrational spectroscopies such as Raman and infrared spectroscopies can be used as a very specific probe of surface-adsorbed molecules, depending on how they are implemented. Since vibrational spectra can readily be simulated by theoretical calculations, by combining theory and spectroscopy it becomes rather easy to identify unambiguously the molecules making up the thin film. The specific technique to use will depend on the desired sensitivity, the information one wants to gather, and the necessity (or lack thereof) to preserve the sample and therefore to use a non-destructive method of analysis. Ideally, when available, Polarization Modulation InfraRed Reflection Absorption Spectroscopy (PM-IRRAS) provides both a non-destructive method and a sensitivity down to the monolayer. This technique, based on polarized infrared light, has the net advantage of only being sensitive to the vibrational modes presenting a non-zero out-of-plane component, and therefore brings also information on the orientation of the molecules in the thin film. This is a non-contact method, and as such, it is a non-destructive method, provided that the samples are handled with care. But such a sophisticated technique is not always readily available. A good alternative, still based on infrared spectroscopy, consists in performing Attenuated Total Reflectance Fourier-Transform InfraRed (ATR-FTIR) spectroscopy. ATR maintains the specificity and most of the sensitivity of PM-IRRAS, but generally does not provide information on the orientation of the molecules. Moreover, it requires the substrate to be in close contact with an ATR crystal, and while this does not formally make it a destructive method, the samples are almost inevitably damaged in the process. Last but not least is Raman spectroscopy. This is a great tool to probe coordination complexes as it frequently allows to detect vibrational modes with rather low wavenumbers, thus providing direct information of the first coordination sphere of the metal. Nevertheless this technique requires the use of an excitation laser to probe the material, and this can cause a few issues, including laser ablation of the thin films, and it should therefore be used with caution.

5.2.3 Optical spectroscopies

Increasing in energy, a whole palette of spectroscopies in the UV-Vis range are useful non-destructive tools. When dealing with transparent substrates (float glass, quartz, conducting ITO), absorption measurements in transmission can be quite sensitive, particularly when extinction coefficients reach very high values, a quite usual feat for coordination complexes, aromatic species or lanthanide derivatives. If absorption bands specific for the film material are present and of sufficient intensity, then both the growth and the nature of the film may be monitored. This can be done in transmission when the substrate is transparent enough in the region of interest, or in reflection when using opaque, highly reflective, smooth metallic substrates. Another popular tool, fluorescence microscopy, benefits from the extreme sensitivity of modern photon detectors, for a moderate cost. The resulting high sensitivity allows the design for example of sensors based on polymeric ultrathin films.[58]

Slightly more confidential, non-linear Second-Harmonic Generation measurements were shown to be useful in the study of LBL Langmuir-Blodgett films (i.e. stacks of LB films).[59] The non-centrosymmetry requirement for the observation of the SHG signal was crafted in the buildup of the film, but beam damage by the pulsed laser is not negligible. While demonstrated thus to be sensitive down to the monolayer level, this technique has not been implemented in further cases.

5.2.4 High-energy-spectroscopies

In the high-energy range of the spectrum, X-ray based spectroscopies are highly sensitive and element specific probes. X-ray Photoemission (XPS) and X-ray Absorption Near-Edge (XANES) spectroscopies are closely related techniques, differing in the mechanism of the reaction between the probed molecule and the incident X-ray beam.[57] Both techniques are technically non-destructive, but require ultra-high vacuum conditions.

On the one hand, laboratory and synchrotron XPS rely on monochromatic incident beams, the photoelectrons ejected from core orbitals of the molecules are collected and their kinetic energies allow to probe the Binding Energies (BEs) of those orbitals. It is element specific, and the BEs of the emission peaks and their integration allow qualitative to quantitative analysis. Variation of the X-ray beam angle of incidence (Angle-Resolved PhotoEmission Spectroscopy, ARPES) allows further characterization of the electronic band structure but may also be used to scan the film along its depth and to gather information on the orientation of the molecules in the film.

On the other hand, XANES is a purely synchrotron-based technique, since it needs the tunability of synchrotron radiation in order to sweep energies around given electronic transitions from core orbitals of a specific element. The cross-section measured for those absorption edges gives then information that is element and oxidation state specific. Moreover selection rules make the technique also sensitive to orbital contributions. The natural polarization of synchrotron light allows to explore that aspect, using circularly polarized light, and also to extract structural information on the orientation of the probed core levels respective to the surface, using linearly polarized light. XANES can be performed as a direct transmission measurement, probing thus the whole depth of the sample, but more often it is performed in Total Electron Yield (TEY) or Fluorescence Yield (FY) detection modes. Those two modes are extremely sensitive, but probe different depths, close to the μm for fluorescence, but down to only a few nm for TEY.

Last but not least in energy, Mössbauer spectroscopy must be evoked, all the more so since it's a tool of choice to study iron derivatives. Sensitivity in the most usual transmission setup is of course limited by the natural abundances of Mössbauer-active isotopes, limited fluxes imposed by handling the radioactivity of standard Mössbauer sources, and of course the natural radioactive decay of those sources that yields rapidly decreasing fluxes. Apart from direct absorption in transmission measurements, other distinct detection modes are possible using the decay paths for the energy of the absorbed γ photon, that end up with high probabilities in ejected photoelectrons. Collection and analysis of the energy of those electrons gives the Conversion Electron Mössbauer Spectroscopy (CEMS). Using channeltrons or XPS-type energy analyzers, this technique becomes sensitive enough to probe ultrathin films of ^{57}Fe.[60] Moreover energy selection of photoelectrons allows depth discrimination and thus a characterization of the profile of the film. A recent evolution of interest has been reached by using the Synchrotron Mössbauer source available at the ID18 beamline of the ESRF. It was shown that this source, obtained by an extreme care in the collimation of the high photon flux of the synchrotron, a multi-step monochromatization and a refinement of the nuclear resonant monochromator obtained with a $^{57}FeBO_3$ single crystal combined with a grazing incidence geometry, allows to investigate thin films down to the single molecular layer.[61] Grazing incidence reflection occurs at the substrate surface, and the molecular layer produces absorption lines that can be treated as those obtained in a standard setup in transmission geometry by correcting the effective thickness of the samples to account for the path lengths of both the incident and reflected radiations inside the molecular layer.

5.3 Study of the photoactive properties of thin films

As mentioned earlier, when switching between LS and HS states, SCO compounds present significant changes in many of their physical properties. Some of those changes can be detected by the very sensitive techniques described above and, bearing some limitations, can allow the study of photo-switchable processes such as LIESST in thin films. One important premise is that while the reduced amount of matter in the film limits severely the choice of techniques, the small effective thickness as compared to the depth penetration of incident light usually ensures much quicker photoconversion as compared to bulk studies.

Methodological issues consist then mainly in: 1) having optical access to the sample, which, depending on the substrate and/or an eventual device configuration, can be limited; 2) keeping down the self-heating due to incident and/or parasite light on the film; 3) prevent laser ablation when using laser light. We will now review the different approaches reported so far.

5.3.1 Magnetometry

Studies of photoinduced states are quite readily done with magnetometers, as described above, but the very small amount of samples present in thin films has rather limited that approach. There are a few reports available on magnetic measurements on films, prepared by the Langmuir-Blodgett technique,[52,53] spin coating,[62] or evaporation.[63,64] Except for the spin-coated film which was only about 30 nm thick, those studies were performed on rather thick films of a few hundreds of nm. The diamagnetic contribution of the substrate is the foremost problem, and for "bulk" measurements, this contribution can be removed by preparing long strips of the thin film on a flexible substrate, typically low-weight diamagnetic Mylar or Kapton polymers. One then rolls the substrate over itself, perpendicularly to the thin film strip, to make a tube small enough to be contained in the standard 5mm diameter plastic straws used for SQUID measurements. This technique allows to go down to 100 nm[64] and probably even less. Nevertheless in that configuration the rolled-up film is not accessible for in situ irradiation. Accordingly the only two reported photomagnetic studies were performed with much thicker films, of which small samples were positioned perpendicularly to an incindent laser light brought by an optical fiber in the SQUID cryostats.[52,63b] In those conditions, the correction of the diamagnetic contribution of the substrate becomes critical and difficult to perform corrrectly.

5.3.2 Scanning probe microscopies and transport measurements

While scanning probe microscopies are usually among the first characterizations performed after the preparation of thin films, and Scanning Tunneling Microscopy/Spectroscopy (STM/STS) is the instrument of choice to study ultrathin films from isolated single-molecules, to a couple of monolayers,[65] they have scarsely been used in combination with in situ irradiation. The main technical issues are of course the difficulty of preventing the overheating of the sample under study, and the possible ablation/displacement of the molecules due to the light. The only reported study has been the beautiful work by Bairagi and coauthors[66] where irradiation was performed through an optical window of the STM using either a LED or a He-Ne laser, with low fluences of 0.2 mW/cm^2, forcing the cryostat to remain below 5 K to cancel out any overheating.

As mentioned STS has been used both to promote the change of spin state and to follow it by changes in the tunneling currents.[65] A related work consisted in studying molecular junctions incorporating SCO thin films of variable thicknesses which transport properties were measured in a classical crossbar junction configuration. The junctions having been grown over a transparent Indium

Tin Oxide electrode on glass, it was possible to access the film optically, and thus to perform measurements in an optical cryostat. This allowed to follow the variation of resistivity of the junctions upon irradiation with a white 100 W halogen lamp.[67] The resistivity variations were seen to correlate with the irradiation.

5.3.3 Vibrational spectroscopies

While infrared and Raman spectroscopies allow to follow SCO in thin films,[55a,68,69,70,71,72,73] they have not been used significantly to characterize photoinduced processes. Raman spectroscopy suffers from various drawbacks, due to the laser excitation required to obtain the Raman resonance. Excitation at power levels necessary to obtain a reasonable signal is expected to cause damages and/or laser ablation in the thin film probed; moreover as explained in *section 2* it can photoexcite the molecules unintentionally when lowering the temperature, as in the only reported study on films grown layer-by-layer.[70] A nice illustration of the latter drawback is shown by the comparison between Raman spectra performed when exciting with red or green light,[74] with a later report showing that actually those wavelengths promoted very efficiently photoconversion to the HS state, thus preventing a correct observation of the LS state.[75] Surprisingly, despite the possibility to perform temperature-dependent measuremnents, no reports so far have been made of the use of PM-IRRAS to follow SCO compounds, whether for thermal or photoinduced conversions.

5.3.4 Optical spectroscopies

Optical spectroscopy presents both the advantage and the inconvenience of needing an optical access to the sample. Irradiation of the sample is thus greatly facilitated, but at the same time the light used to probe the sample and obtain the spectra may also end up photocommuting the sample, as pointed out above for Raman spectroscopy. This is all the more an issue for ultrathin films where light absorption is expected to be negligible. Sensitivity will depend very much on the nature of the absorption band probed and its corresponding extinction coefficient. As mentioned in *section 2.2*, SCO is accompanied by changes in the absorption bands corresponding to electronic transitions with metal contribution, most explicit with d-d type transitions, but also affects Charge Transfer bands, usually located around 400-600 nm for bands with Metal-to-Ligand Charge Transfer character. The much higher extinction coefficients of the latter type, typically 10^4 M^{-1} cm^{-1}, can be used to follow the spin state for nanometric thin films prepared on transparent substrates, as reported on dropcast films.[69,71] The use of an auxiliary laser in a classical pump-probe configuration allows then to characterize photoexcitation processes on Langmuir-Blodgett films,[52] and on evaporated films.[74,76] The same procedure can be also followed for reflectance measurements, which is particularly useful for devices where the SCO film is covered by another layer, e.g. an electrode.[67]

Another optical method particularly adapted for thin film studies is Surface Plasmon Resonance (SPR). It has been used to evidence the change of spin state for drop-cast/stamped films close to room temperature,[71,77] but the compounds studied do not show photocommutation at low temperature. Such a study would certainly have been very challenging, SPR relying on a precise adjustment of refractive indices in the sensing crystal, that may not be amenable to cooling down to cryogenic temperatures.

5.3.5 High-energy spectroscopies

XPS, and even more XANES, are undoubtedly the most efficient and precise techniques for studying the change of spin state of thin, to ultrathin, to submonolayer films. Those techniques

relying on soft X-ray and photoelectrons emission/collection require rigourous Ultra-High Vacuum conditions, which in itself put some limitations on the materials that can be studied. Most often the films studied were prepared by evaporation, ideally performed in situ for synchrotron-based XANES experiments. Nevertheless, transparent ports with glass or quartz windows are usually available, which allow *in-situ* irradiation with white light or laser light. One must consider that the distance between the port and the sample is typically on the order of 30-40 cm, so it is advisable to use a collimator, either with lenses adapted to the wavelength of choice, or reflective collimators that are more broadband (Figure 6). Spots of a few mm at that distance can then be easily focused to cover all of the samples to photoexcite.

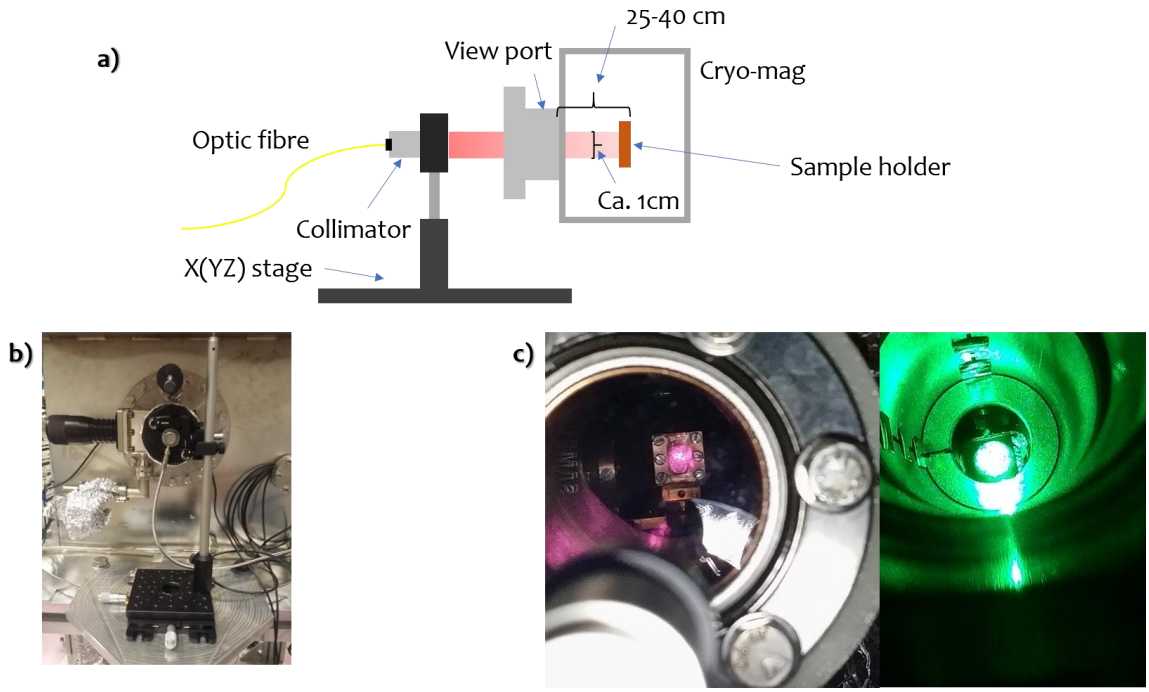

***Figure 6**. a) scheme of a typical setup for photoirradiation in a UHV chamber; b) reflective collimator used on the cryomagnet at ID32, ESRF; c) pictures of in-situ laser spots on sample holders in the UHV cryostats at the XAS beamlines DEIMOS, SOLEIL, and ID32, ESRF.*

The most important issue is nevertheless the interaction with the synchrotron X-ray beam. Since we are dealing with molecular species that are usually not very resistant to high-fluence radiation (or high fluxes of photoelectrons, which results still from high X-ray fluences), special care must be taken to avoid "burning" the molecules, by limiting fluences either with an absorber, typically a thin metal or plastic foil, or by slightly defocusing the optics between the monochromator and the sample chamber. Another related issue is the so-called SOft X-ray Induced Excited Spin State Trapping (SOXIESST), the apparent population of the metastable HS state at low temperature caused by the incident X-ray beam. Quite logically, it has been shown that this effect is in fact the occurrence of a classical LIESST effect, for which the excitation is caused by photoelectrons in the optical energy range.[78] Ideally, to prevent this effect, the beam must be attenuated, which can be done satisfactorily mainly when working in TEY detection mode, with ultra-low noise cryostats combined with high-performance electrometers.

While quantitative interpretation of Fe 2p XPS spectra is delicate, due to the various pathways available for the photoelectrons, attenuation/reabsorption problems, etc.. Fe $L_{2,3}$ edge XANES can

provide rather easily a quantitative assessment of the LS/HS ratio, provided one has available reference spectra of pure LS and HS states, that are used as a basis set for a linear interpolation procedure.[79] The relatively easy optical access therefore allows to perform studies under light irradiation using external light sources such as white lamps or laser diodes, and has allowed to study the LIESST effect in a variety of samples. But in all cases, care must be taken to assess for the occurrence of SOXIESST, as this usually unwanted photoelectron induced phenomenon can compete directly with the desired LIESST[78c] effect induced by irradiation.[63c] When this confounding effect is taken into account, it is nevertheless possible to establish photo-conversion kinetics, or to estabish whether the photo-excited HS states correspond to the thermally induced ones. This approach has been consistently pursued these last few years on a variety of molecules and substrates.[55c,63c,76c,80] Amongst the most surprising results reported with this technique was the observation of LIESST on an evaporated film when nothing was observed on the powder of the complex,[80c] and the dependence of SOXIESST on the polarization of a ferroelectric substrate.

To conclude with high-energy techniques, we can mention the Synchrotron Mössbauer source, which was recently used to study ultrathin films of two different SCO complexes.[81] Photocommutation was studied with an original arrangement of the lights sources, which were commercial low-cost LEDs. Those LEDs were tested previously at 5K to ascertain the center of the emission spectrum. The LEDs were then mounted in-situ on the sample holder (see Figure 7), and current-controlled through leads brought outside of the cryostat. LIESST could be observed on 5nm thin films with satisfying sensitivity. These promising results could pave the way to further similar studies.

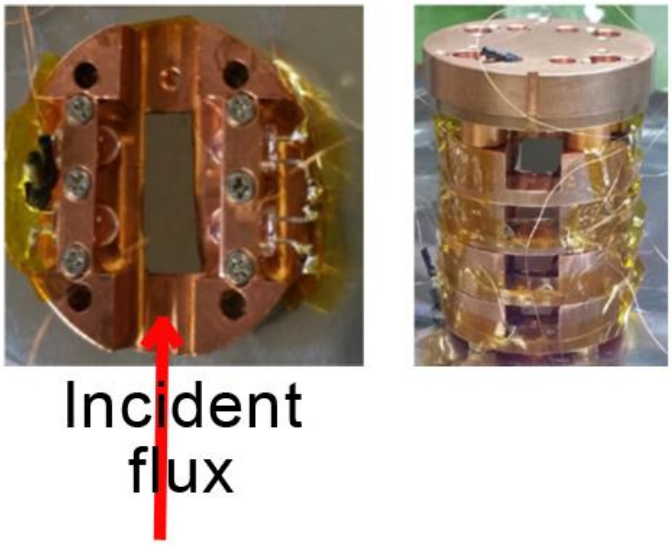

Figure 7. *Top (a) and side (b) views of the modified sample holders with LEDs and connections.*

Conclusion

As presented in this chapter, many techniques can be used to characterize spin crossover compounds, and their light-induced switching. Each of them is a probe of a specific change occurring along the SCO and is then complementary to all the other techniques. They all require cautions in order to know exactly the sample that is characterized (morphology, composition…) and the relevant information available using such techniques without over interpretating the data.

Acknowledgement
The authors would like to thanks all their collaborators for the great scientific and friendly exchanges and all the students that have contributed to the increase of knowledge. All the financial support are also acknowledged: CNRS, University of Bordeaux, Région Nouvelle Aquitaine, ANR, Soleil and ESRF facilities.

Permissions
Every author has a responsibility to gain permissions for any figures/tables they wish to include that have already been published. This also includes artwork that have previously been published by Elsevier, as although there will be no charge permission still needs to be gained. To request permission please go to: http://www.copyright.com/

Abbreviations of ligands
bbtr = 1,4-di(1,2,3-triazol-1-yl)butane
4,4'-bipy = 4,4'-bipyridine
3ditz = 1,3-bis-(1*H*-tetrazol-1-yl)propane
Hpy-DAPP = {bis[N-(2-pyridylmethyl)-3-aminopropyl](2-pyridylmethyl)amine}
Htrz = 1,2,4-4*H*-triazole
L = {(3,3')-[1,2-phenylenebis(iminomethylidyne)]bis(2,4-pentanedionato)(2–)-N,N',O^2,$O^{2'}$}
Lpz = N,N'-dimethyl-N,N'-bis((pyrazin-2-yl)methyl)-1,2-ethanediamine
3-OCH_3-SalEen is the Schiff-base produced from the condensation of 3-methoxysalicylaldehyde and *N*-ethyl-ethylenediamine
phen = 1,10-phenanthroline;
pic = picoline
PM-PEA = N-(2'-pyridylmethylene)-4-(phenylethynyl)aniline
ptz = 1-propyltetrazole

References

1 Chastanet, G.; Lorenc, M.; Bertoni, R.; Desplanches, C. *C. R. Chimie* **2018**, *21*, 1075-1094.
2 (a) Boillot, M.-L.; Zarembowitch, J.; Sour, A. *Top. Curr. Chem*. **2004**, *234*, 261-276; (b) Brachnakova, B.; Salitros, I. *Chem. Papers*, **2018**, *72*, 773-798.
3 (a) Dommaschk, M.; Gutzeit, F.; Boretius, S.; Haag, R.; Herges, R. *Chem. Commun*. **2014**, 12476-12479; (b) Lochenie, C.; Wagner, K. G.; Karg, M.; Weber, B. *J. Mater. Chem. C* **2015**, *3*, 7925-7935; (c) Dommaschk, M.; Peters, M.; Gutzeit, F.; Schütt, C.; Näther, C.; Sönnichsen, F.D.; Tiwari, S.; Riedel, C.; Boretius S.; Herges, R. *J. Am. Chem. Soc*. **2015**, *137*, 7552-7555.
4 (a) Decurtins, S.; Gutlich, P.; Kohler, C. P.; Spiering, H.; Hauser, A. *Chem. Phys. Lett.* **1984**, *105*, 1-4; (b) Hauser, A.; Gütlich, P. *Comprehensive Coordination Chemistry II*, **2003**, *2*, 427-434.
5 (a) Shimamoto, N.; Ohkoshi, S.; Sato, O.; Hashimoto, K.; *Chem. Lett.* **2002**, 486-487; (b) Freysz, E.; Montant, S.; Létard, S.; Létard, J.-F. *Chem. Phys. Lett.* **2004***, 394*, 318-323; (c) Bonhommeau, S.; Molnar, G.; Galet, A.; Zwick, A.; Real, J.A.; McGarvey, J.J.; Bousseksou, A. *Angew. Chem. Int. Ed. Engl.* **2005**, *44*, 4069-4073; (d) Collet, E.; Henry, L.; Pineiro-Lopez, L.; Toupet, L.; Real, J.A. *Curr. Inorg. Chem*. **2016**, *6*, 61-66; (e) Fouché, O.; Dégert, J.; Jonusauskas, G.; Daro, N.; Létard, J.-F.; Freysz, E. *Phys. Chem. Chem. Phys* **2010***, 12*, 3044-3052; (f) Castro, M.; Roubeau, O.; Pineiro-Lopez, L.; Real, J.A.; Rodriguez-Velamazan, J.A. *J. Phys. Chem. C* **2015***, 119*, 17334-17343; (g) Gallé,

G.; Etrillard, C.; Degert, J.; Guillaume, F.; Létard, J.-F.; Freysz, E. *Appl. Phys. Lett.* **2013**, *102*, 063302(1-4); (h) Hellel, W.; Ould Hamouda, A.; Degert, J.; Letard, J.-F.; Freysz, E. *Appl. Phys. Lett*. **2013**, *103*, 143304(1-5); (i) Freysz, E.; Létard, J.-F. *French patent* **2012** FR 2993978-A1.

6 (a) Hendrickson, D.N.; Pierpont, C.G. *Top. Curr. Chem*. **2004**, *234,* 63-95; (b) Dei, A.; Gatteschi, D.; Sangregorio, C.; Sorace, L. *Acc. Chem. Res*. **2004**, *37*, 827-835; (c) Tezgerevska, T.; Alley, K.G.; Boskovic, C. *Coord. Chem. Rev*. **2014**, *268*, 23-40; (d) Evangelio, E.; Ruiz-Molina, D. *C.R. Chimie*, **2008**, *11*, 1137-1154.

7 (a) Sato, O.; Iyoda, T.; Fujishima, A.; Hashimoto, K. *Science* **1996**, *272*, 704-5; (b) Bleuzen, A.; Marvaud, V.; Mathoniere, C.; Sieklucka, B.; Verdaguer, M. *Inorg. Chem*. **2009**, *48*, 3453-3466; (c) Ohkoshi, S.; Tokoro, H. *Acc. Chem. Res.* **2012**, *45*, 1749-1758; (d) Aguila, D.; Prado, Y.; Koumousi, E.S.; Mathoniere, C.; Clérac, R. *Chem. Soc. Rev*. **2016**, *45*, 203-224; (e) Mathoniere, C.; Tokoro, H.; Ohkoshi, S.-I. in *Molecular Magnetic Materials: Concepts and Applications*, **2017** Ed. B. Sieklucka, D. Pinkowicz, Wiley-CVH, 323.

8 Zerdane, S.; Cammarata, M.; Balducci, L.; Bertoni, R.; Catala, L.; Mazerat, S.; Mallah, T.; Pedersen, M.N.; Wulff, M.; Nakagawa, K.; Tokoro, H.; Ohkoshi, S.-I.; Collet, E. *Eur. J. Inorg. Chem* **2018,** 272-277.

9 Costa, J. S. *C. R. Chimie* **2018**, *21*, 1121-1132.

10 Collet, E.; Guionneau, P. *C. R. Chimie* **2018**, *21*, 1133-1151.

11 Wolny, J. A.; Schünemann, V.; Németh, Z.; Vanko, G. *C. R. Chimie* **2018**, *21*, 1152-1169.

12 Sorai, M. *Top. Curr. Chem*. **2004**, *235*, 153-170.

13 (a) Homenya, P. ; Heyer, L. ; Renz, F. *Pure. Appl. Chem*. **2015**, *87*, 293-300; (b) Hauser, A. *Top. Curr. Chem.* **2004**, *234*, 155-198; (c) Bertoni, R.; Cammarata, M.; Lorenc, L. ; Matar, S.F. ; Létard, J.-F. ; Lemke, H.T. ; Collet, E. *Acc. Chem. Res*. **2015**, *48*, 774-781.

14 (a) Tribollet, J.; Galle, G.; Jonusauskas, G.; Deldicque, D.; Tondusson, M.; Létard, J.-F.; Freysz, E. *Chem. Phys. Lett*. **2011**, *513*, 42-47; (b) Consani, C.; Prémont-Schwarz, M.; El Nahhas, A.; Bressler, C.; van Mourik, F.; Cannizzo, A.; Chergui, M. *Angew. Chem. Int. Ed. Engl*. **2009**, *48*, 7184-7187; (c) Bressler, C.; Milne, C.; Pham, V.-T.; El Nahhas, A.; van der Veen, R.M.; Gawelda, W.; Johnson, S.; Beaud, P.; Grolimun, D.; Kaiser, M.; Borca, C.N.; Ingold, G.; Abela, R.; Chergui, M. *Science*, **2009**, *323*, 489-492; (d) Degert, J.; Lascoux, N.; Montant, S.; Létard, S.; Freysz, E.; Chastanet, G.; Létard, J.-F. *Chem. Phys. Lett*. **2005**, *415*, 206-210..

15 Legrand, V.; Pillet, S.; Souhassou, M.; Ligan, N.; Lecomte, C. *J. Am. Chem. Soc*. **2006**, *128*, 13921-13931.

16 Hauser, A. *Chem. Phys. Lett*. **1986**, *124*, 543-548.

17 (a) Tuchagues J.-P., Bousseksou A., Molnár G., McGarvay J. J., Varret F., *Top. Curr. Chem.* **2004**, 235, 85-103; (b) Wolny J. A., Diller R., Schünemann V., *Eur. J. Inorg. Chem.* **2012**, 2635-2648.

18 Sorai M., Seki S., *J. Phys. Chem. Solids* **1974**, 35, 555-570.

19 Müller D., Knoll C., Seifried M., Weinberg P., *Vibrational Spectroscopy* **2016**, 86, 198-205.

20 Haddad M. S., Federer W. D., Lynch M. W., Hendrickson D. N., *Inorg. Chem.* **1981**, 20, 131-139.

21 Köning E., Ritter G., Kulshreshtha S. K., Csatary N., *Inorg. Chem.***1984**, 23, 1903-1910.

22 Weber B., Kaps E. S., Desplanches C., Létard J.-F., *Eur. J. Inorg. Chem.* **2008**, 2963-2966.

23 Paradis N., Le Gac F., Guionneau P., Largeteau A., Yufit D. S., Rosa P., Létard J.-F., Chastanet G., *Magnetochemistry* **2016**, 2, 15(1-17).

24 Herber H., Casson L. M., *Inorg. Chem.* **1986**, 25, 847-852.

25 Buron-Le Cointe M., Ould Moussa N., Trzop E., Moréac A., Molanr G., Toupet L., Bousseksou A., Létard J.-F., Matouzenko G., *Phys. Rev. B* **2010**, 82, 214106(1-11).

26 Guillaume F., Tobon Y. A., Bonhommeau S., Létard J.-F., Moulet L., Freysz E., *Chem. Phys. Let*. **2014**, 604, 105-109.

27 Lever A . B. P. *Inorganic Electronic Spectroscopy* 2nd Edition **1986** Studies in physical and theoretical chemistry 33, Elsevier, Amsterdam.

28 Hauser A. Ligand field theoretical considerations *Top. Curr. Chem.* **2004**, *233*, 49-58.

29 Decurtins, S.; Gutlich, P.; Hasselbach; Hauser, A.; Spiering, H. *Inorg. Chem.* **1985**, *24* 2174-2178.

30 Chakraborty, P.; Bronisz, R.; Besnard, C.; Guénée, L.; Pattison, P.; Hauser, A. *J. Am. Chem. Soc.* **2012**, *134*, 4049-4052.

31 Goodwin, H. *Top. Curr. Chem*., **2004**, *233*, 59-94

32 Phan, H. V.; Chakraborty, P. Chen, M.; Calm, Y. M.; Kovnir, K.; Keniley Jr., L. K.; Hoyt, J. M.; Knowles, E. S. ; Besnard, C.; Meisel, M. W.; Hauser, A.; Achim, C.; Shatruk, M. *Chem. Eur. J.* **2012**, *18*, 15805-15815.

33 Shores, M. P., Klug, C. M., Fiedller, S. R. in *Spin Crossover Materials: Properties and Applications*, 1st edition, M. A. Halcrow, **2013**, John Wileys & Sons, Ltd.

34 Morscheidt, W.; Codjovi, E.; Jeftic, J.; Linarès, J.; Bousseksou, A.; Constant-Machado, H. ; Varret, F. *Meas. Sci. Techn.* **1998**, *9,* 1311-1317.

35 Liu, X.; Zhou, J.; Bao, X.; Yan, Z.; Guo, P; Rouzières, M.; Mathonière, C.; Liu, J.-L.; Clérac, R. *Inorg. Chem.,* **2017,** *56*, 12148-12157.

36 Toulemonde, O. ; Devoti, A. ; Rosa, P. ; Guionneau, P. ; Duttine, M. ; Wattiaux, A. ; Lebraud, E. ; Penin, N. ; Decourt, R. ; Fargues, A. ; Buffière, S. ; Demourgues, A. ; Gaudon, M. *Dalton Trans.* **2018**, *47*, 382-393.

37 Enachescu C., Constant-Machado H., Codjovi E., Linares J., Boukheddaden K, Varret F., *J. Phys. Chem. Solids* 2001, *62*, 1409-1422.

38 Létard J.-F., Chastanet G., Guionneau P., Desplanches C., in *Spin Crossover Materials: Properties and Applications*, Ed. Malcom A. Halcrow, John Wilfreysey & sons, 475, **2013**.

39 (a) Bartual-Murgui C., Natividad E., Roubeau O., *J. Mater. Chem. C* **2015**, 3, 7916-7924; (b) Gimenez-Marqués M., Garcia-Sanz de Larrea M. L., Coronado E., *J. Mater. Chem. C* 2015, 3, 7946-7953; (c) Grosjean A., Daro N., Pechev S., Etrillard C., Chastanet G., Guionneau P., *Eur. J. Inorg. Chem.* **2018**, 429-434; (d) Daro N., Moulet L., Penin N., Paradis N., Létard J.-F., Lebraud E., Buffière S., Chastanet G., Guionneau P., *Materials* **2017**, 10, 60(1-13); (e) Manrique-Juárez M. D., Suleimanov I., Hernández E. M., Salmon L., Molnár G., Bousseksou A., *Materials* **2016**, 9, 537(1-9); (f) Dugay J., Giménez-Marqués M., Kozlova T., Zandbergen H. W., Coronado E., van der Zant H. S. J., *Adv. Mater.* **2015**, *27*, 1288-1293.

40 Guionneau P., *Dalton Trans*. **2014**, *43*, 382-393 (c) Halcrow, M. A. *Chem. Soc. Rev.* **2011**, *40*, 4119-4142 (d) Shatruk, M.; Phan, H.; Chrisostomo, B. A.; Suleimenova, A. *Coord. Chem. Rev*. **2015**, *289*, 62-73 (e) Pfaffeneder, T.A.; Thallmair, S.; Bauer, W.; Weber, B. *New J. Chem*. **2011**, *35*, 691-700

41 (a) Pillet, S.; Bendeif, E.; Bonnet, S.; Shepherd, H.J.; Guionneau, P. *Phys. Rev. B* **2012**, *86*, 064106(1-11) (b) Buron-Le Cointe, M.; Hébert, J.; Baldé, C.; Moisan, N.; Toupet, L.; Guionneau, P.; Létard, J.F.; Freysz, E.; Cailleau, H.; Collet, E. *Phys. Rev. B* **2012**, *85*, 064114(1-4) (c) Trzop, E.; Buron-Le Cointe, M.; Cailleau, H.; Toupet, L.; Molnar, G.; Bousseksou, A.; Gaspar, A.B.; Real, J.A.; Collet, E. *J. Appl. Cryst.* **2007**, *40*, 158-164 (d) Guionneau, P.; Collet, E. in: *Spin-Crossover Materials*, John Wiley & Sons Ltd, **2013**, pp. 507-526 (e) Legrand, V.; Pillet, S.; Weber, H.P.;

Souhassou, M.; Létard, J.F.; Guionneau P.; Lecomte, C.. *J. Appl Cryst*., **2007**, *40*, 1076-1088; (f) Craig, G.A.; Costa, J.S.; Roubeau, O.; Teat, S.J.; Shepherd, H.J.; Lopes, M.; Molnár, G.; Bousseksou, A.; Aromí, G. *Dalton Trans*., **2014**, *43*, 729-737 (g) Sheu, C.-F.; Chen, K.; Chen, S.-M.; Wen, Y.-S.; Lee, G.-H.; Chen, J.-M.; Lee, J.-F.; Cheng, B.-M.; Sheu, H.-S.; Yasuda, N.; Ozawa, Y.; Toriumi, K.; Wang, Y. *Chem. Eur. J.* **2009**, *15*, 2384-2393. (h) Marchivie, M.; Guionneau, P.; Howard, J.A.K.; Chastanet, G.; Létard, J.F.; Goeta A.E.; Chasseau, D. *J. Am. Chem. Soc.*, **2002**, *124*, 194

42 (a) Howard, J.A.K.; Probert, M.R. *Science* **2014**, *343*, 1098-1102. (b) Als-Nielsen, J., McMorrow, D. *Elements of modern X-ray physics*, Wiley, New York, **2001**. (c) Hammond C. *The Basics of Crystallography and Diffraction*, IUCr Texts on Crystallography 3, Oxford University Press, **1997**. (d) Giacovazzo C. *Fundamentals of Crystallography* Oxford Univ. Press, Oxford, ed. 3, **2003**.

43 Pillet, S.; Legrand, V.; Weber, H.P.; Souhassou, M.; Létard, J.F.; Guionneau P.; Lecomte, C. *Z. Kristallogr.*, **2008**, *223*, 235-249.

44 (a) Unruh, D.; Homenya, P.; Kumar, M.; Sindelar, R.; Garcia, Y.; Renz, F. *Dalton Trans*., **2016**, *45*, 14008-14018 (b) Vank, G., Renz, F.; Molnar, G.; Neisius, T.; Karpati, S. *Angew. Chem. Int. Ed*. **2007**, *46*, 5306 –5309 (c) Bhattacharjee, A.; Kusz, J.; Zubko, M.; Goodwin, H.A.; Gütlich, P. *J. Molec. Struct.* **2008**, *890*, 178–183.

45 (a) Wilson, C.C. *Crystallography Reviews*, **2009**, *15*, 3-56; (b) Goeta, A.E.; Howard, J.A.K. *Chem Soc Rev.* **2004**, *33*(8), 490-500.

46 (a) Tao, J.; Wei, R.-J.; Huang, R.-B.; Zheng, L.-S. *Chem. Soc. Rev.* **2012**, *41*, 703-737 (b) Thorarinsdottir, A.E.; Gaudette, A.I.; Harris, T.D. *Chem. Sci.* **2017**, *8*, 2448-2456; (c) Phonsri, W., Davies, C.G., Jameson, G.N.L., Moubaraki, B., Murray, K.S. *Chem. Eur. J.* **2016**, *22*, 1322-1333. (d) Matouzenko, G.S.; Jeanneau, E.; Verata, A.Y.; Bousseksou, A. *Dalton Trans.* **2011**, *40*, 9608-9618. (e) Sheu, C.-F.; Pillet, S.; Lin, Y.-C.; Chen, S.-M.; Hsu, I-J.; Lecomte, C.; Wang Y. *Inorg. Chem*. **2008**, *47*, 10866-10874. (f) Quesada, M.; de la Pena-O'Shea, V. A.; Aromi, G.; Geremia, S.; Massera, C.; Roubeau, O.; Gamez, P.; Reedijk, J. *Adv. Mater*. **2007**, *19*, 1397–1402.

47 Guionneau, P.; Lakhloufi, S.; Lemée-Cailleau, M.H.; Chastanet, G.; Rosa, P.; Mauriac, C.; Létard, J.F. *Chem. Phys. Lett.* 2012, *542*, 52–55.

48 Marchivie, M.; Guionneau, P.; Letard, J.-F.; Chasseau, D.; Howard, J.A.K. *J. Phys. Chem. Solids* 2004, 65, 17–23

49 (a) Ozawa, Y.; Pressprich, M. R.; Coppens, P. *J. Appl. Cryst*. **1998**, *31*, 128-135; (b) Kim, C. D.; Pillet, S.; Wu, G.; Fullagar, W. K.; Coppens, P. *Acta Cryst*. **2002**, *A58*, 133-137. (c) Huby, N.; Guérin, L.; Collet, E.; Toupet, L.; Ameline J.-C.; Cailleau, H.; Roisnel, T.; Tayagaki, T.; Tanaka, K. *Phys. Rev. B* **2004**, *69*, 020101.

50 (a) Cailleau, H.; Lorenc, M.; Guérin, L.; Servol, M.; Collet, E.; Buron-Le Cointe, M. *Acta Cryst.* **2010**, *A66*, 189-197. (b) Collet, E.; Boillot, M.L.; Hebert, J.; Moisan, N.; Servol, M.; Lorenc, M.; Toupet, L.; Buron-Le Cointe, M.; Tissot, A.; Sainton, J. *Acta Cryst*. **2009**, *B65*, 474-480. (c) Marino, A.; Buron-Le Cointe, M.; Lorenc, M.; Toupet, L.; Henning, R.; DiChiara, A.D.; Moffat, K.; Brefuel, N.; Collet, E. *Faraday Discuss*. **2015**, *177*, 363-379.

51 (a) Bousseksou, A.; Molnár, G.; Salmon, L.; Nicolazzi, W. *Chem. Soc. Rev.* **2011**, *40*, 3313–3335; (b) Cavallini, M. *Phys. Chem. Chem. Phys.* **2012**, *14*, 11867-11876; (c) Mallah, T.; Cavallini, M. *C. R. Chim.* **2018**, *21*, 1270–1286.

52 Létard, J. F.; Nguyen, O.; Soyer, H.; Mingotaud, C.; Delhaès, P.; Kahn, O. *Inorg. Chem.* **1999**, *38*, 3020–3021.

53 Soyer, H.; Dupart, E.; Gómez-García, C. J.; Mingotaud, C.; Delhaès, P. *Adv. Mater.* **1999**, *11* (5), 382–384.

54 Denawi, H.; Koudia, M.; Hayn, R.; Siri, O.; Abel, M. *J. Phys. Chem. C* **2018**, *122* (26), 15033–15040.

55 (a) Cobo, S.; Molnár, G.; Real, J. A.; Bousseksou, A. *Angew. Chemie - Int. Ed.* **2006**, *45* (35), 5786–5789; (b) Bartual-Murgui, C.; Salmon, L.; Akou, A.; Thibault, C.; Molnár, G.; Mahfoud, T.; Sekkat, Z.; Real, J. A.; Bousseksou, A. *New J. Chem.* **2011**, *35* (10), 2089; (c) Rubio-Giménez, V.; Bartual-Murgui, C.; Galbiati, M.; Núñez-López, A.; Castells-Gil, J.; Quinard, B.; Seneor, P.; Otero, E.; Ohresser, P.; Cantarero, A.; Coronado, E.; Real, J. A.; Mattana, R.; Tatay, S.; Martí-Gastaldo, C. *Chem. Sci.* **2019**, *10*, 4038–4047; (d) Sakaida, S.; Otsubo, K.; Sakata, O.; Song, C.; Fujiwara, A.; Takata, M.; Kitagawa, H. *Nat. Chem.* **2016**, *8* (4), 377–383.

56 (a) Poneti, G.; Poggini, L.; Mannini, M.; Cortigiani, B.; Sorace, L.; Otero, E.; Sainctavit, P.; Magnani, A.; Sessoli, R.; Dei, A. *Chem. Sci.* **2015**, *6* (4), 2268–2274 ; (b) Mannini, M.; Poggini, L. *Encycl. Interfacial Chem.* **2018**, 538–546.

57 Cornia, A.; Mannini, M.; Sainctavit, P.; Sessoli, R. *Chem. Soc. Rev.* **2011**, *40* (6), 3076–3091.

58 (a) Muller, M.; Langmer, A.; Krylova, O.; Le Moal, E.; Sokolowski, M. *Appl. Phys. B: Lasers and Optics*, **2011**, *105*, 67-79; (b) Shinzaburo, I.; Hiroyuki, A. *Bull. Chem. Soc. Japan,* **2003**, *76*, 1693-1705.

59 (a) Le Breton, H.; Létard, J. F.; Lapouyade, R.; Le Calvez, A.; Maleck Rassoul, R.; Freysz, E.; Ducasse, A.; Belin, C.; Morand, J. P. *Chem. Phys. Lett.* **1995**, *242* (6), 604–616; (b) Desrousseaux, S.; Bennetau, B.; Morand, J.; Mingotaud, C.; Létard, J.-F.; Montant, S.; Freysz, E. *New J. Chem.* **2000**, *24*, 977–985.

60 Kajcos, Z.; Meisel, W.; Kuzmann, E.; Tosello, C.; Gratton, M. L.; Vértes, A.; Gütlich, P.; Nagy, D. L. *Hyperfine Interact.* **1990**, *57*, 1883–1888.

61 Cini, A.; Mannini, M.; Totti, F.; Fittipaldi, M.; Spina, G.; Chumakov, A.; Rüffer, R.; Cornia, A.; Sessoli, R. *Nat. Commun.* **2018**, *9* (1).

62 Matsuda, M.; Tajima, H. *Chem. Lett.* **2007**, *36* (6), 700–701.

63 (a) Shi, S.; Schmerber, G.; Arabski, J.; Beaufrand, J.-B.; Kim, D. J.; Boukari, S.; Bowen, M.; Kemp, N. T.; Viart, N.; Rogez, G.; Beaurepaire, E.; Aubriet, H.; Petersen, J.; Becker, C.; Ruch, D. *Appl. Phys. Lett.* **2009**, *95*, 043303; (b) Palamarciuc, T.; Oberg, J. C.; El Hallak, F.; Hirjibehedin, C. F.; Serri, M.; Heutz, S.; Létard, J.-F.; Rosa, P. *J. Mater. Chem.* **2012**, *22*, 9690-9695; (c) Davesne, V.; Gruber, M.; Studniarek, M.; Doh, W. H.; Zafeiratos, S.; Joly, L.; Sirotti, F.; Silly, M. G.; Gaspar, A. B.; Real, J. A.; Schmerber, G.; Bowen, M.; Weber, W.; Boukari, S.; Da Costa, V.; Arabski, J.; Wulfhekel, W.; Beaurepaire, E. *J. Chem. Phys.* **2015**, *142*, 1–9.

64 Poggini, L.; Gonidec, M.; González-Estefan, J. H.; Pecastaings, G.; Gobaut, B.; Rosa, P. *Adv. Electron. Mater.* **2018**, *4*, 1800204.

65 (a) Gopakumar, T. G.; Matino, F.; Naggert, H.; Bannwarth, A.; Tuczek, F.; Berndt, R. *Angew. Chemie - Int. Ed.* **2012**, *51* (25), 6262–6266; (b) Miyamachi, T.; Gruber, M.; Davesne, V.; Bowen, M.; Boukari, S.; Joly, L.; Scheurer, F.; Rogez, G.; Yamada, T. K.; Ohresser, P.; Beaurepaire, E.; Wulfhekel, W. *Nat. Commun.* **2012**, *3*, 936–938; (c) Gruber, M.; Davesne, V.; Bowen, M.; Boukari, S.; Beaurepaire, E.; Wulfhekel, W.; Miyamachi, T. *Phys. Rev. B* **2014**, *89*, 195415/1-5; (d) Jasper-Tönnies, T.; Gruber, M.; Karan, S.; Jacob, H.; Tuczek, F.; Berndt, R. *J. Phys. Chem. Lett.* **2017**, *8*, 1569–1573; (d) Knaak, T.; González, C.; Dappe, Y. J.; Harzmann, G. D.; Brandl, T.; Mayor, M.; Berndt, R.; Gruber, M. *J. Phys. Chem. C* **2019**, *123*, 4178–4185.

66 Bairagi, K.; Iasco, O.; Bellec, A.; Kartsev, A.; Li, D.; Lagoute, J.; Chacon, C.; Girard, Y.; Rousset, S.;

Miserque, F.; Dappe, Y. J. ; Smogunov, A.; Barreteau, C.; Boillot, M.-L.; Mallah, T.; Repain, V. *Nat. Commun.* **2016**, *7*, 1–7.

67 Lefter, C.; Rat, S.; Costa, J. S.; Manrique-Juárez, M. D.; Quintero, C. M.; Salmon, L.; Séguy, I.; Leichle, T.; Nicu, L.; Demont, P.; Rotaru, A.; Molnár, G.; Bousseksou, A. *Adv. Mater.* **2016**, 7508–7514.

68 Soyer, H.; Mingotaud, C.; Boillot, M.-L.; Delhaes, P. *Langmuir* **1998**, *14*, 5890–5895.

69 Kuroiwa, K.; Shibata, T.; Sasaki, S.; Ohba, M.; Takahara, A.; Kunitake, T.; Kimizuka, N. *J. Polym. Sci. Part A Polym. Chem.* **2006**, *44*, 5192–5202.

70 Agustı, G.; Cobo, S.; Gaspar, A. B.; Szila, P. Á.; Vieu, C.; Mun, M. C.; Real, A.; Bousseksou, A. *Thin Films.* **2008**, 6721–6732.

71 Gural'skiy, I. A. *J. Nanophotonics* **2012**, *6*, 063517.

72 Shalabaeva, V.; Rat, S.; Manrique-Juarez, M. D.; Bas, A.-C.; Vendier, L.; Salmon, L.; Molnár, G.; Bousseksou, A. *J. Mater. Chem. C* **2017**, *5*, 4419–4425.

73 Bartual-Murgui, C.; Cerf, A.; Thibault, C.; Vieu, C.; Salmon, L.; Molnár, G.; Bousseksou, A. *Microelectron. Eng.* **2013**, *111*, 365–368.

74 Naggert, H.; Rudnik, J.; Kipgen, L.; Bernien, M.; Nickel, F.; Arruda, L. M.; Kuch, W.; Tuczek, F. *J. Mater. Chem. C* **2015**, *3*, 7870–7877.

75 Rat, S.; Mikolasek, M.; Costá, J. S.; Chumakov, A. I.; Nicolazzi, W.; Molnár, G.; Salmon, L.; Bousseksou, A. *Chem. Phys. Lett.* **2016**, *653*, 131–136.

76 (a) Naggert, H.; Bannwarth, A.; Chemnitz, S.; von Hofe, T.; Quandt, E.; Tuczek, F. *Dalton Trans.* **2011**, *40*, 6364; (b) Ludwig, E.; Naggert, H.; Kalläne, M.; Rohlf, S.; Kröger, E.; Bannwarth, A.; Quer, A.; Rossnagel, K.; Kipp, L.; Tuczek, F. *Angew. Chemie - Int. Ed.* **2014**, *53*, 3019–3023; (c) Ossinger, S.; Naggert, H.; Kipgen, L.; Jasper-Toennies, T.; Rai, A.; Rudnik, J.; Nickel, F.; Arruda, L. M.; Bernien, M.; Kuch, W.; Berndt, R.; Tuczek, F. *J. Phys. Chem. C* **2017**, *121*, 1210–1219

77 Félix, G.; Abdul-Kader, K.; Mahfoud, T.; Guralskiy, I. A.; Nicolazzi, W.; Salmon, L.; Molnár, G.; Bousseksou, A. *J. Am. Chem. Soc.* **2011**, *133*, 15342–15345.

78 (a) Davesne, V.; Gruber, M.; Miyamachi, T.; Da Costa, V.; Boukari, S.; Scheurer, F.; Joly, L.; Ohresser, P.; Otero, E.; Choueikani, F.; Gaspar, A. B.; Real, J. A.; Wulfhekel, W.; Bowen, M.; Beaurepaire, E. *J. Chem. Phys.* **2013**, *139*, 1–6; (b) Kipgen, L.; Bernien, M.; Nickel, F.; Naggert, H.; Britton, A. J.; Arruda, L. M.; Schierle, E.; Weschke, E.; Tuczek, F.; Kuch, W. *J. Phys. Condens. Matter* **2017**, *29*, aa7e52; (c) Wäckerlin, C.; Donati, F.; Singha, A.; Baltic, R.; Decurtins, S.; Liu, S.-X.; Rusponi, S.; Dreiser, J. *J. Phys. Chem. B* **2018**, *122*, 8202–8208.

79 (a) Warner, B.; Oberg, J. C.; Gill, T. G.; El Hallak, F.; Hirjibehedin, C. F.; Serri, M.; Heutz, S.; Arrio, M.; Sainctavit, P.; Mannini, M.; Poneti, G.; Sessoli, R.; Rosa, P.; *J. Phys. Chem. Lett.* **2013**, *4* , 1–23; (b) Bernien, M.; Wiedemann, D.; Hermanns, C. F.; Krüger, A.; Rolf, D.; Kroener, W.; Müller, P.; Grohmann, A.; Kuch, W. *J. Phys. Chem. Lett.* **2012**, *3*, 3431–3434; (c) Bernien, M.; Naggert, H.; Arruda, L. M.; Kipgen, L.; Nickel, F.; Miguel, J.; Hermanns, C. F.; Kru, A.; Kru, D.; Tuczek, F.; Kuch, W. *ACS Nano* **2015**, *9*, 8960–8966; (d) Gopakumar, T. G.; Bernien, M.; Naggert, H.; Matino, F.; Hermanns, C. F.; Bannwarth, A.; Mühlenberend, S.; Krüger, A.; Krüger, D.; Nickel, F.; Walter, W.; Berndt, R.; Kuch, W.; Tuczek, F. *Chem. - A Eur. J.* **2013**, *19*, 15702–15709; (e) Schleicher, F.; Studniarek, M.; Kumar, K. S.; Urbain, E.; Katcko, K.; Chen, J.; Frauhammer, T.; Herve, M.; Halisdemir, U.; Kandpal, L. M.; Lacour, D.; Riminucci, A.; Joly, L.; Scheurer, F.; Gobaut, B.; Choueikani, F.; Otero, E.; Ohresser, P.; Arabski, J.; Schmerber, G.; Wulfhekel, W.; Beaurepaire, E.; Weber, W.; Boukari, S.; Ruben, M.; Bowen, M. *ACS Appl. Mater.* **2018**, *10*, 31580–31585

80 (a) Poggini, L.; Milek, M.; Londi, G.; Naim, A.; Poneti, G.; Squillantini, L.; Magnani, A.; Totti, F.; Rosa, P.; Khusniyarov, M. M.; Mannini, M. *Mater. Horizons* **2018**, *5* (3), 506–513; (b) Atzori, M.; Poggini, L.; Squillantini, L.; Cortigiani, B.; Gonidec, M.; Bencok, P.; Sessoli, R. *J. Mater. Chem. C* **2018**, *6* (L), 8885–8889; (c) Rohlf, S.; Gruber, M.; Flöser, B. M.; Grunwald, J.; Jarausch, S.; Diekmann, F.; Kalläne, M.; Jasper-Toennies, T.; Buchholz, A.; Plass, W.; Berndt, R.; Tuczek, F.; Rossnagel, K. *J. Phys. Chem. Lett.* **2018**, *9* (7), 1491–1496; (d) Bairagi, K.; Bellec, A.; Fourmental, C.; Iasco, O.; Lagoute, J.; Chacon, C.; Girard, Y.; Rousset, S.; Choueikani, F.; Otero, E.; Ohresser, P.; Sainctavit, P.; Boillot, M.-L.; Mallah, T.; Repain, V. *J. Phys. Chem. C* **2018**, *122* (1), 727–731

81 Cini, A.; Poggini, L.; Chumakov, A.; Spina, G.; Fittipaldi, M.; Wattiaux, A.; Dutine, M.; Rosa, P.; Mannini, M. *manuscript in preparation*